Airway Bacteria Drive a Progressive COPD-Like Phenotype in Mice with Polymeric Immunoglobulin Receptor Deficiency

By

Bradley Winston Richmond

Dissertation

Submitted to the Faculty of the

Graduate School of Vanderbilt University

in partial fulfillment of the requirements

for the degree of

DOCTOR OF PHILOSOPHY

in

Cell and Developmental Biology

May, 2017

Nashville, Tennessee

Approved:

Timothy S. Blackwell, M.D.

Robert J. Coffey, M.D.

James R. Goldenring, M.D., Ph.D.

Emily Hodges, Ph.D.

William P. Tansey, Ph.D.

To my wife, Anna, for her love and endurance

and

my sons Carter and Wyatt, pride of my life.

ACKNOWLEDGEMENTS

This year marks the 10th anniversary of my graduation from medical school and arrival at Vanderbilt. It has been an exhilarating, tumultuous, and defining decade that has exceeded my wildest expectations as a new medical school graduate. I have been professionally and personally blessed by so many individuals during this period that summarizing my appreciation in a short dissertation acknowledgments section seems like an injustice. But I won't turn down the opportunity.

I thank Dr. Brian Ernsting, my undergraduate molecular biology teacher, for challenging me to pursue a career in science. Yes, people do this all the time Brian, and now I'm one of those people. I thank Dr. John Newman, whose letter of support brought me to Vanderbilt and back to my home to continue my clinical and scientific training. John is still around, and I hope he is glad he wrote that letter. I thank Dr. Wonder Drake, who carefully tended the first sparks of my career as a physician-scientist. Wonder's outrageous overestimation of my abilities gave me the confidence to pursue this career path, and she continues to serve as a standard bearer for who I want to be as a physician, scientist, and person.

Most of all I thank my mentor Dr. Tim Blackwell. In 2012, Tim and I sat down and he said, "Let me tell you a story we've been working on in mucosal immunity and COPD." Every day I come to work hoping to turn another page of that story. While Tim's scientific acumen is readily apparent to all who interact with him, there are other qualities which I have come to appreciate as equally important to his success as a physician-scientist. His willingness to listen carefully to the opinions of others, to identify and focus energy on the things that really matter, and to remain patient and steadfast in times of difficulty are the qualities I have come to admire most. Tim, I am profoundly grateful to have had a chance to train under your guidance these past four years and hope I can one day be half the mentor you are.

I would like to thank the members of my thesis committee, Dr. Bob Coffey, Dr. Jim Goldenring, Dr. Emily Hodges, and Dr. Bill Tansey. Your feedback challenged me to ask better questions and provided valuable advice to help me answer them. I am particularly thankful to Bob and Jim who coordinate the epithelial pathobiology course, which provided training in stem cell and epithelial biology at a critical time in the evolution of my project. I am also thankful for my committee's forbearance as I balanced my clinical responsibilities with my doctoral work. This was new territory for all of us, and I think it went as well as could be expected. In addition to my thesis committee, my work benefitted from input from my divisional research advisory committee, which consisted of Dr. Pierre Massion and Dr. Stokes Peebles. I appreciate the scientific and career advice I've received from both of you. Countless other mentors – many of which would not want to be identified as such – have provided inspiration, encouragement, and advice at key junctures: Dr. Julie Bastarache, Dr. William Lawson, Dr. Scott Smith, Dr. Todd Hulgan, Dr. Jon Kropski, and many others. If it takes a village to raise a child, it takes a city to raise a physician-scientist.

I am most appreciative to many current and former members of the Blackwell Lab for their expertise, friendship, and patience. In particular I would like to thank Dr. Vasiliy Polosukhin, whose vision and dedication established the scientific foundation for this work. Vasiliy is unrelenting in his demand for excellence, but demands the most from himself. I am indebted to Dr. Rui-Hong Du who patiently taught me many of the techniques required in this dissertation and continues to serve as a thoughtful colleague and friend. Other members have the lab have helped in a myriad of ways: Linda Gleaves, Taylor Sherrill, Wei Han, Rasul Abdolrasulnia, Pierre Hunt, Dong-Sheng Cheng, Yongqin Zhang, Allison Perry, Ankita Burman, Jamie Saxon, Rinat Zaynagetdinov, Mindy McConaha, Hari Tanjore, Sergey Novitskiy, and many more.

Lastly, I am thankful to my family. My parents Rick and Janet Richmond are not scientists by vocation, but instilled in me an appreciation for the beauty of the natural world, an

analytic approach to problem solving, and above all a stubborn tenacity that has served me well in this career. My wife of nearly eight years, Anna, has been an unwavering source of love and support. Anna, how you have managed to support my career so well while working multiple jobs, completing your own doctoral degree, and raising two boisterous boys is a continued source of amazement. I am proud of what we have accomplished together. Finally, I thank my sons Carter and Wyatt, who have refocused my priorities and made me a better person. My prayer is that both of you will one day find work as fulfilling to you as mine has been to me.

TABLE OF CONTENTS

LIST OF FIGURES

LIST OF ABBREVIATIONS

AECOPD	acute exacerbation of chronic obstructive pulmonary disease
AEE	apical early endosome
AGER	advanced glycosylation end product-specific receptor
ALI	air-liquid interface
ANOVA	analysis of variance
ARE	apical recycling endosome
ASL	airway surface liquid
BAL	bronchoalveolar lavage
BEE	basolateral early endosome
CCSP	Clara cell secretory protein
CHRNA3/5	cholinergic nicotine receptor alpha
CMV	cytomegalovirus
COPD	chronic obstructive pulmonary disease
CS	cigarette smoke
CSE	cigarette smoke extract
DAPI	4',6-diamidino-2-phenylindole, dihydrochloride
dIgA	dimeric immunoglobulin A
EBV	Epstein-Barr virus
FAM13A	family with sequence similarity 13, member A
FEV1	forced expiratory volume in 1 second
FISH	fluorescent in situ hybridization
FRβ	folate receptor beta
GWAS	genome-wide association study
H&E	hematoxylin and eosin

HBECS	human bronchial epithelial cell
HHIP	hedgehog-interacting protein
HNF	hepatic necrosis factor
IFN	interferon
IgA	immunoglobulin A
IL	interleukin
IREB2	iron regulatory binding protein 2
IRF	interferon regulatory factor
IT	intratracheal
MCC	multiciliated cell
MLI	mean linear intercept
MMP	matrix metalloproteinase
MTEC	murine tracheal epithelial cell
NE	neutrophil elastase
NF-κB	nuclear factor kappa B
NTHi	non-typeable *Haemophilus influenzae*
OTU	operational taxonomic unit
PAS	periodic acid-Schiff
PBS	phosphate-buffered saline
PCR	polymerase chain reaction
pIgR	polymeric immunoglobulin receptor
RER	rough endoplasmic reticulum
SC	secretory component
SERPINA1	serpin family A member 1
SIgA	secretory immunoglobulin A

TGN	trans-Golgi network
VNAM	vancomycin, neomycin, ampicillin, and metronidazole
VV_{airway}	subepithelial connective tissue volume density
WT	wild-type

I. INTRODUCTION

Impact, clinical manifestations, and risk factors for COPD

Chronic obstructive pulmonary disease (COPD) is a common and highly morbid respiratory disorder that is closely associated with long-term exposure to tobacco smoke. COPD is now the third leading cause of death in the United States and globally and was estimated to account for over $32 billion in direct healthcare expenditures in 2010 (1-3). Symptoms of COPD include dyspnea, chronic cough, and excess sputum production (4). The diagnosis of COPD is made when individuals displaying these symptoms are found by spirometry to have irreversible obstruction to expiratory airflow (4). Affected individuals develop increasingly severe exertional dyspnea that may progress to include resting dyspnea, chronic hypoxic and/or hypercarbic respiratory failure, and death in 35-67% of patients (5, 6). In addition, patients with COPD are at risk for sudden increases in dyspnea, cough, and sputum production termed acute exacerbations of COPD (AECOPD). The annual rate of COPD exacerbations has been estimated at 0.5-3.5 per patient, and these exacerbations are associated with decreased quality of life, accelerated decline in lung function, and increased mortality (5, 7-10).

The main risk factor for the development of COPD is chronic exposure to tobacco smoke. In industrialized countries, the population-attributable risk for smoking as a cause for COPD is estimated at 77-84% for men and 61-62% for women, depending on age (11). In addition to tobacco smoke exposure, exposure to air pollution is also thought to contribute to COPD risk (12). In developing countries, indoor air pollution due to combustion of biomass fuels and coal is an important risk factor for COPD, particularly in women (13, 14).

Smokers with a first-degree relative with COPD have an increased risk of developing the disease, suggesting that genetic factors play a role in disease susceptibility (15). Indeed, inactivating mutations in *SERPINA1* (serpin family A member 1), the gene encoding the

antiprotease alpha-1-antitrypsin, were first identified as a cause for pulmonary emphysema in 1963 (16). Using data from genome-wide association studies (GWAS), Zhou and colleagues estimated the total heritability of COPD at 38% (17). GWAS studies have identified and validated several risk loci for COPD phenotypes including *CHRNA3/5* (cholinergic nicotine receptor alpha), *IREB2* (iron regulatory binding protein 2), *HHIP* (hedgehog-interacting protein), *FAM13A* (family with sequence similarity 13, member A), and *AGER* (advanced glycosylation end product-specific receptor) (18-23). However, unlike mutations in *SERPINA1*, the biological mechanism through which these single nucleotide polymorphisms contribute to COPD remain unknown, and the effect size of individual alleles for disease risk is small.

Histopathology of COPD

Airflow obstruction in COPD results from the combined effects of multiple anatomic lesions, including abnormalities in small airways, large airways, and the lung parenchyma (24). Small airways disease is the earliest disease manifestation in COPD and accounts for the majority of airflow obstruction (25, 26). Pathological changes observed in small airways in

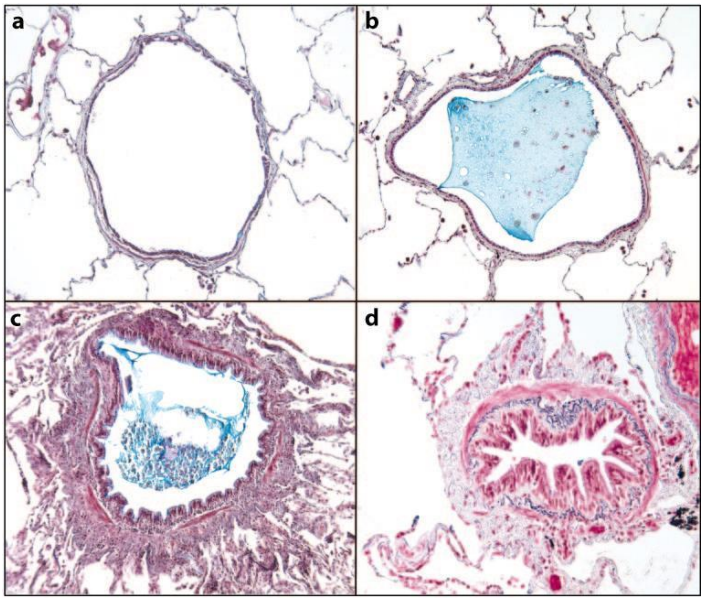

Figure 1: Histopathology of small airways disease in COPD.

A) A normal small airway shown for comparison. **B**) An airway with the lumen partially filled with a bland mucus plug containing a few epithelial cells. **C**) A small airway with an active inflammatory process, where the exudate extends into the lumen. **D**) A small airway that has been narrowed by collagen deposition in the peribronchiolar space. Adapted from Hogg et al. (24) with permission. Copyright © 2009 Annual Reviews.

COPD include altered epithelial differentiation, mucus plugging, smooth muscle hyperplasia, immune/inflammatory cell accumulation, and fibrotic remodeling of the airway wall (**Figure 1**) (24, 27-29). Together, these changes result in narrowing of small airways and obliteration and dropout of up to 90% of small airways in severe disease (30). Centroacinar emphysema, the form primarily associated with cigarette smoke exposure, develops in proximity to diseased airways and results from alveolar wall cell death and/or failure of alveolar wall maintenance (31, 32). This results in a loss of elastic recoil in the lung, which contributes to airflow obstruction (33). The physical proximity of centrilobular emphysema to small airways has led to speculation that injurious substances produced by inflammatory cells recruited to small airways promotes emphysematous lung destruction (34). Large airways disease is also common in COPD, and commonly observed lesions include smooth muscle hyperplasia, submucosal gland hypertrophy and hyperplasia, and alterations in epithelial morphology such as goblet cell hyperplasia (35). Together, these abnormalities result in increased mucus production which can also contribute to airflow obstruction.

The protease/antiprotease model of COPD pathogenesis

In 1963, Laurell and Eriksson reported congenital deficiency of the antiprotease alpha-1-antitrypsin as a cause for early-onset pulmonary emphysema (36). Alpha-1-antitrypsin is a serine protease inhibitor that is produced in the liver but accumulates in the lung, where it inhibits proteolytic enzymes such as neutrophil elastase (37). Shortly after Laurell and Eriksson's seminal finding, Gross et al. showed that intratracheal instillation of papain caused pulmonary emphysema in rats (38). Additional experiments confirmed and extended this observation to show that a variety of enzymes capable of degrading elastin cause emphysema in animal models (39-43). Further, it was found that transgenic mice lacking macrophage or neutrophil-derived elastase were protected from cigarette-smoke induced emphysema (44, 45). These findings suggested that emphysematous lung destruction in COPD occurs when

proteases produced by inflammatory cells recruited to cigarette smoke-exposed airways overwhelm local antiprotease production, a model which came to be known as the protease-antiprotease hypothesis (46, 47). While the protease-antiprotease model provided an explanation for how cigarette smoke damages the lung, this model failed to explain why patients with COPD continue to have inflammation in the lung and an accelerated decline in lung function after smoking cessation (48, 49). Defects in efferocytosis and autoimmune responses have been proposed as stimuli for continued inflammation after smoking cessation (50-52).

Structure of the airway epithelium in health and in COPD

The observation that small airways disease is the earliest anatomic lesion in COPD (25) has resulted in increased scrutiny on how alterations in the structure of the respiratory epithelium in small airways might contribute to COPD pathogenesis. In humans, airways > 1 mm in diameter are lined by a pseudostratified epithelium composed primarily of multiciliated cells, secretory cells, and basal cells (53). The secretory cell lineage is further divided into goblet and Club (formerly Clara) cells, with goblet cells predominating in large airways and Club cells in small airways (54). These cell types function in a coordinated manner to maintain the integrity of the respiratory epithelium, replenish cells lost due to normal turnover, and repopulate the epithelium in response to injury (53). Multiciliated cells (MCCs) each contain several hundred cilia, which beat in a coordinated fashion to move inhaled irritants trapped in mucins (produced by goblet cells) toward the posterior oropharynx, where they are swallowed (55, 56). Club cells predominate in the lower airways and produce a variety of substances including Clara cell secretory protein (CCSP) and anti-proteinases. Basal cells derive their name from the fact that they are located near the basement membrane in pseudostratified epithelium. Lineage-tracing experiments in mice have shown that basal cells are capable of self-renewal and can differentiate into ciliated and secretory lineages (57), and thus these cells are considered to be the main progenitor cell for the respiratory epithelium. However, there is substantial plasticity

among cell types in the pulmonary epithelium, and transdifferentiation among ciliated, Club, and basal cells has been documented in animal models in response to injury (58, 59). This may be particularly important for repopulation in the distal airways (<1 mm), where a simple cuboidal epithelium dominates and cells displaying typical basal cell markers are rare.

Structural changes in the respiratory epithelium in COPD include basal cell hyperplasia, loss of ciliated cells, goblet cell hyperplasia, and squamous metaplasia (60, 61). In severe COPD, up to 80% of small airways are covered by structurally abnormal epithelium (61). Functional consequences for these changes include a dysfunctional mucociliary escalator, reduced epithelial integrity, formation of mucus plugs, and reduced regenerative capacity (27, 62-64). In addition, abnormal epithelial differentiation has been associated with loss of secretory immunoglobulin A (SIgA) in the small airways of patients with COPD (**Figure 2**) (61).

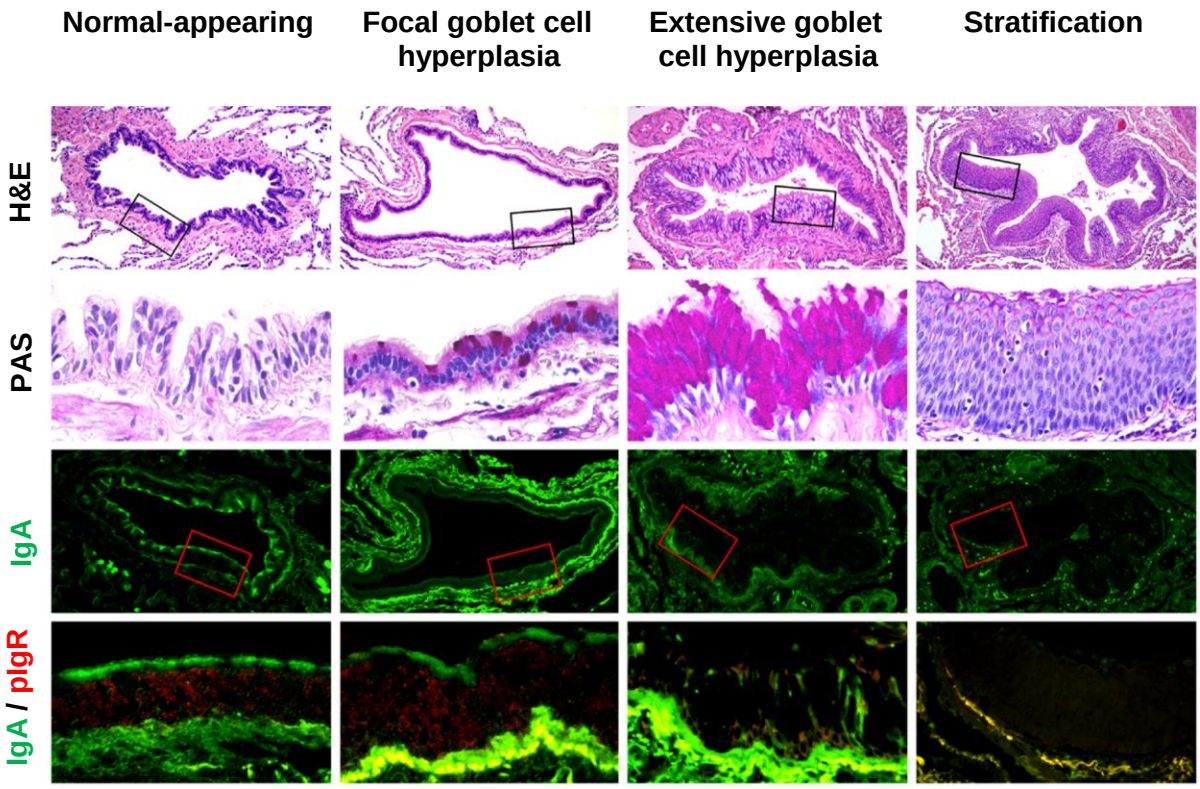

Figure 2: Spectrum of pathologic changes in the small airways of COPD patients.

Top row: Hematoxylin and eosin (H&E)-stained 5 micron lung sections showing the range of pathologic changes in the small airways of COPD patients (x100). **Row 2**: Periodic acid-Schiff (PAS)-stained lung sections highlight mucus-producing (predominantly goblet) cells in the area depicted in the small box in the top row (x400). **Row 3 and 4**: Epithelial remodeling is associated with reduced expression of pIgR and decreased SIgA transport to the mucosal surface (x100; insets x400). Adapted from Polosukhin et al. (61) with permission. Copyright © 2016 American Thoracic Society. The American Journal of Respiratory and Critical Care Medicine is an official journal of the American Thoracic Society.

Barrier function of the airway epithelium

Since the mucosal surface of airways is continuously exposed to an array of particulates and microorganisms, an intricate set of defenses is required to prevent bacterial invasion and limit inflammatory responses to bacteria and inhaled irritants (65-67). In addition to maintaining mucociliary clearance, epithelial cells form tight junctions and maintain a thin airway surface liquid (ASL) layer that contains a number of epithelial-derived antimicrobial substances (65-68). In addition to these non-specific defense mechanisms, epithelial cells regulate mucosal immunity by controlling airway delivery of SIgA, which consists of two IgA monomers and secretory component (SC) joined by a J chain (69, 70). Dimeric IgA (dIgA) is produced by plasma cells in the submucosa, and can bind to membrane-bound polymeric immunoglobulin receptor (pIgR) at the basolateral surface through formation of a disulfide bond (69). Bound pIgR/dIgA complexes are endocytosed, transported to the apical surface of the cell, and then released into the ASL through an endoproteolytic cleavage event in the pIgR (**Figure 3**). The portion of the pIgR that remains bound to dIgA is then referred to as SC, and the SC-dIgA complex is referred to as SIgA. dIgA/pIgR complexes can neutralize intracellular antigens during transcytosis and facilitate their release into the ASL, or cleaved SIgA may bind airway antigens after release into the ASL (69). While the IgA portion of SIgA provides antigen-specific responses, the SC contributes a variety of non-specific antimicrobial functions including protecting IgA from degradation by host and microbial proteases, improving bacterial adherence, and modulating host inflammatory factors (71). Through a process known as immune exclusion, SIgA agglutinates airborne antigens and microorganisms, preventing them from activating or injuring airway epithelial cells (72-74).

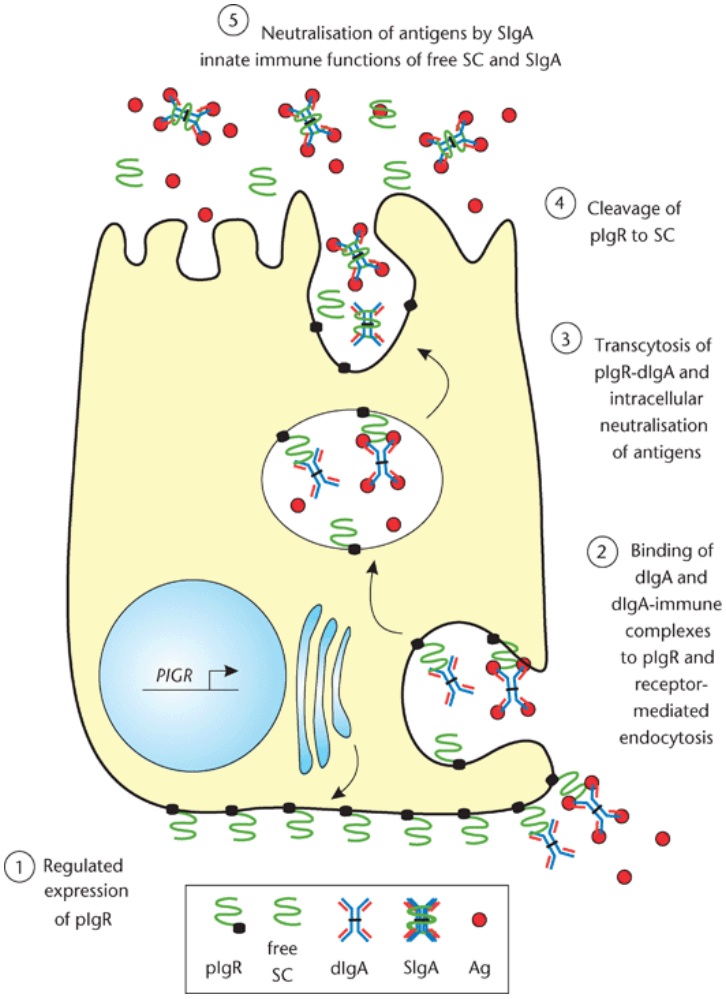

Figure 3: Transport of dIgA/pIgR through the airway epithelium to form SIgA.

After synthesis as an integral membrane protein in the rough endoplasmic reticulum (RER), pIgR enters the Golgi apparatus and is packaged into vesicles in the *trans*-Golgi network (TGN). These vesicles are targeted to the basolateral membrane through interactions between residues in a 17 amino acid portion of the carboxy-terminal cytoplasmic domain and adaptor coat proteins such as AP-1 (**Step 1**) (75-77). pIgR may undergo spontaneous clathrin-mediated endocytosis, or may form a disulfide bond with dIgA which dramatically increases the rate of transcytosis (**Step 2**). Endocytosis is mediated by phosphorylation of tyrosine and serine residues on pIgR, via activation of $p62^{Yes}$, and by hydrolysis of Rab3b (78-81). Following endocytosis, pIgR/dIgA complexes are delivered first to basolateral early endosomes (BEEs) and then to apical recycling endosomes (AREs) in a microtubule-dependent process (82). During intracellular transport, dIgA can bind and neutralize intracellular antigens (**Step 3**). At the apical surface, an endoproteolytic cleavage event releases a portion of pIgR (the secretory component or SC) and dIgA into the ASL, together forming SIgA (**Step 4**). SIgA can then neutralize airway antigens present in the ASL (**Step 5**). A small amount of pIgR is recaptured at the apical membrane and recycled via apical early endosomes (AEEs) (82). Adapted with permission from Kaetzel (83).

Function of SIgA in the gut

Whereas the role of SIgA in the respiratory epithelium has only recently been investigated (61, 67, 84-88), the importance of SIgA in maintaining mucosal homeostasis in the gut has been well-studied and extensively reviewed (69, 71, 72, 89, 90). Up to 3 g of SIgA is produced by the intestinal epithelium each day (91, 92). The majority of this IgA is germline-encoded, low affinity, and cross-reactive with numerous bacterial antigens; however, in response to bacterial challenge, plasma cells in the lamina propria can produce specific, high-affinity IgA antibodies through somatic hypermutation (93). This dual-capability helps SIgA promote tolerance to commensal intestinal bacteria in homeostatic conditions while contributing to a robust immune response in response to bacterial challenge (71, 73, 94). $pIgR^{-/-}$ mice, which lack SIgA at all mucosal surfaces, have increased susceptibility to bacterial infection in multiple body sites, highlighting the importance of SIgA in prevention of infection (95-97). While immune exclusion is thought to represent the primary mechanism through which SIgA maintains mucosal homeostasis, it is important to note that during transit across the airway epithelium vesicle-bound SIgA can neutralize viruses including HIV (69, 71). Conversely, some viruses and bacteria may hijack pIgR/SIgA to gain entry into deeper tissues (98, 99).

In addition to preventing infection, SIgA helps to maintain tolerance with the mucosal microbiome, and mice and humans with defective SIgA secretion show increased susceptibility to inflammatory bowel and celiac disease (100, 101). $pIgR^{-/-}$ mice have been shown to have a less diverse total colonic microbiota but a more diverse adherent microbiota, suggesting that SIgA prevents outgrowth of select bacterial species while preventing bacteria from adhering to the mucosal epithelium (90). Additionally, the affinity of IgA differs between bacteria, and influences the composition of the intestinal microbiome in health and disease (102-107). Conversely, the luminal microbiome modulates IgA levels both through regulation of *PIGR* expression and through degradation. *PIGR* expression is upregulated by NF-κB activation,

which results from bacterial activation of Toll-like and other pattern recognition receptors. MyD88-deficient mice, which have diminished NF-κB responses to bacteria, have decreased pIgR expression and SIgA transcytosis compared to WT littermates (108). Further, *in vivo* studies suggest that the composition of the gut microbiome modulates intestinal SIgA levels through variable production of bacterial proteases capable of cleaving SIgA (101).

II. QUESTIONS ADDRESSED BY THIS DISSERTATION

Role of SIgA in mucosal homeostasis of the lung

In contrast to the gut, the role that SIgA plays in maintaining mucosal homeostasis in the airways has only recently begun to be investigated. Pilette and colleagues first reported that reduced SC (the portion of the pIgR that remains bound to IgA) is reduced in the airways of patients with COPD and that lower levels of SIgA correlate with increased disease severity (85). Subsequently, Polosukhin et al. reported that loss of SIgA in individual airways is associated with increased bacterial invasion, NF-κB pathway activation, increased numbers of airway neutrophils and macrophages, and fibrotic airway wall remodeling (109). Based on these findings, we hypothesize that SIgA deficiency may contribute to protease/antiprotease imbalance in COPD and provide an explanation for ongoing lung damage in patients with COPD who no longer smoke. We propose that in airways with abnormal epithelial differentiation, loss of SIgA predisposes the airway epithelium to bacterial invasion, which in turn activates inflammatory signaling pathways in airway epithelial cells. This results in recruitment of neutrophils and macrophages, which produce proteases that contribute to protease/antiprotease imbalance and lung damage. Further, we propose that once remodeling and loss of SIgA are established, chronic inflammation due to bacterial invasion acts to perpetuate abnormal differentiation within small airways. In this manner, a cycle of inflammation, abnormal epithelial remodeling, and lung damage is established that may persist after smoking cessation.

In Chapter IV of this dissertation, we will utilize an animal model of SIgA deficiency to determine whether SIgA deficiency plays a causal role in COPD pathogenesis and establish whether airway bacteria are the primary stimulus for continued inflammation in SIgA-deficient airways. Additional experiments will explore whether loss of SIgA modulates the lung microbiome in the lung as has been shown in the gut (102-105) and whether loss of SIgA augments lung damage induced by cigarette smoke. In Chapter V of this dissertation, we will

use this same model to explore whether repetitive bacterial challenge increases lung inflammation and damage in SIgA-deficient airways above levels induced by endogenous bacteria, and whether anti-inflammatory treatment can prevent lung damage induced by repetitive bacterial challenge.

Mechanism of reduced SIgA in the airways of patients with COPD

In Chapter VI of this dissertation, we will change our focus to examine why pIgR expression is reduced in the small airways of patients with COPD. Polosukhin et al. previously reported that reduced SIgA in the airways of patients with COPD results from reduced *PIGR* transcription in remodeled airways (61). This finding was later confirmed by Gohy and colleagues, who also showed that reduced *PIGR* expression by human bronchial epithelial cells (HBECs) isolated from patients with COPD persists *in vitro* in air-liquid interface (ALI) culture (87). Because transcytosis of each molecule of dIgA across the airway epithelium requires a molecule of pIgR, reduced *PIGR* expression will necessarily result in reduced transport of dIgA across the airway epithelium, assuming an excess of dIgA relative to pIgR.

Basal expression of *PIGR* is regulated in part through binding of upstream stimulatory factor (USF) 1 and 2 and activator protein 2 (AP2) to an E-box motif at position -71 (-74 in mice) (69, 110, 111). *PIGR* expression can be markedly upregulated through binding of inflammatory transcription factors including interferon regulatory factor (IRF) 1 and 3, STAT6, NF-κB, and HNF-1 (69), which may be directly induced through activation of Toll-like and PRRs or indirectly via inflammatory cytokines such as IL-4, IFN-γ, and TNF (112-114). COPD is an inflammatory disease characterized by increases in IL-4, TNF, and several other pro-inflammatory cytokines (115, 116). Thus, it is likely that decreased expression of *PIGR* in COPD patients results from a loss of pIgR-expressing cells in remodeled airway rather than reduced transcription of *PIGR* in individual cells. Evidence for this was again provided by Gohy et al., who found that *PIGR* was

reduced in the airways patients with severe COPD relative to controls, but increased in the airways of smokers without airway remodeling (87).

Given that airway remodeling in COPD is generally associated with a loss of multiciliated cells, we speculate that these cells are the primary source of pIgR in the airway epithelium, and thus play a unique role in maintaining epithelial homeostasis. In Chapter VI, we provide evidence that the differentiation factor p73, recently shown to be critical for the development of multiciliated cells (117, 118), is required for pIgR expression. Additional studies show that CS suppresses p73 expression *in vitro* and *in vivo*, potentially through an NF-κB-dependent mechanism, and that p73 is reduced in the airways of patients with COPD.

III. MATERIAL AND METHODS FOR CHAPTERS IV AND V

Animal models

pIgR$^{-/-}$ mice, backcrossed onto a C57Bl/6 background for a minimum of 8 generations (119), were obtained from the Mutant Mouse Resource Research Center at the University of Missouri. WT and pIgR$^{-/-}$ mice were housed in standard microisolator cages in a centralized animal care facility and provided food and water *ad libitum*. Germ-free mice pIgR$^{-/-}$ were surgically derived by sterile embryo transfer and maintained in sterile flexible film Trexler isolators at the National Gnotobiotic Rodent Resource Center (University of North Carolina School of Medicine, Chapel Hill, NC). Within Trexler isolators, mice were housed in standard microisolator cages with sterilized bedding and provided with sterilized rodent chow and water *ad libitum*. Sterility was documented on a monthly basis by fecal Gram stain, aerobic and anaerobic cultures, and polymerase chain reaction (PCR) for 16s rRNA of the feces and bedding. For selected mice, sterility of feces was also documented by Gram stain and cultures at the time of necropsy. For all experiments male and female mice were sacrificed from age 2-12 months and compared to age-matched WT mice as indicated. For the microbiome and germ-free experiments, WT and germ-free mice were housed together. For all other experiments, WT and pIgR$^{-/-}$ were housed separately. All procedures involving mice were approved by the Institutional Care and Use Committee of Vanderbilt University.

In vivo treatments

WT or pIgR$^{-/-}$ mice were exposed to mainstream cigarette smoke (CS) from two 3R4F research cigarettes (Center for Tobacco Reference Products, University of Kentucky) once daily for two weeks, followed by four 3R4F cigarettes twice daily until sacrifice at 8 months. Cigarettes were smoked sequentially, one 5 second puff/minute for a total of 7 puffs/cigarette, using a nose-only exposure system (inExpose, Scireq, Montreal, CA). Control animals were

housed in identical nose-only cages but were exposed to filtered air only. For NTHi nebulization studies, mice were placed in a whole-body nebulization chamber (inExpose, Scireq) and exposed to 10 mg of aerosolized NTHi lysate delivered by a 5 L/min pump. Control animals were treated with aerosolized phosphate-buffered saline (PBS). For repetitive nebulization experiments, mice were treated with 10 mg of aerosolized NTHi lysate once weekly for 4 months. All animals were harvested 4 days after the final nebulization treatment. For the SIgA pretreatment experiment, one hour prior to nebulization, 50 μL of a 0.34 mg/mL solution of IgA from pooled human colostrum (Sigma-Aldrich) or 50 μL sterile PBS was administered intratracheally after intubation of isofluorane-anesthetized mice.

Roflumilast administration

For studies using roflumilast, 200 μL of 0.5 mg/mL suspension of roflumilast or vehicle (4% methylcellulose, 1.3% PEG400, ~ 5 μg drug/mg animal weight) was administered by oral gavage once daily, 5 days/week for the duration of treatment. The roflumilast suspension was freshly prepared each week and stored at 4°C.

Preparation of NTHi lysates

NTHi strain 1479 (a gift from Dr. Brahm Segal, University of Buffalo) was grown overnight on chocolate agar plates (Hardy Diagnostics, Santa Maria, CA) and then used to inoculate 20 mL of brain-heart infusion media (Sigma-Aldrich, St. Louis, MO) containing 10 μg/mL nicotinamide adenine dinucleotide and 10 μg/mL Hemin (both from Sigma-Aldrich). The culture was incubated for 4 hours at 36°C with constant shaking and then used to inoculate an additional 200 mL of liquid media. After another 4 hours of growth, bacteria were pelleted, boiled for one hour, sonicated twice for one minute each, and filtered through a 0.22 μM polyethylsulfone filter (EMD Millipore, Darmstadt, Germany) using 1 mL of added PBS for each

pellet generated from 50 mL of liquid culture. Protein concentration was adjusted to 1.5 mg/mL in PBS using Bradford assay (Pierce, Rockford, IL).

Lung harvest technique and BAL

After perfusion with normal saline, the left lung was isolated, removed, and flash-frozen in liquid nitrogen, while the right lung was inflated using a 25-cm pressure column containing 10% neutral buffered formalin. The frozen left lungs were stored at −80^{o}C and used for protein analyses. The right lungs were fixed overnight in 10% formalin and then embedded in paraffin for histological analyses. Bronchoalveolar lavage (BAL) was performed using two 500 μL aliquots of sterile PBS. Fluid was combined and centrifuged at 400 *g* for 10 min. to separate cells from supernatant. Supernatant was stored at −80°C and then used for cytokine and chemokine measurements. Separate animals were utilized for histological analyses and BAL.

Histology and immunohistochemistry

5 μm serial sections were cut from each tissue specimen and H&E and Masson trichrome staining was performed. Additional serial sections were used for immunostaining with rabbit polyclonal anti-IgA (#PAB9360, Abnova, Taipei City, Taiwan; 1:100) to detect SIgA on airway epithelial surface, rabbit polyclonal anti-neutrophil elastase (#ab68672, Abcam; 1:200) to detect neutrophils, rabbit polyclonal anti-CD68 (#ab125512, Abcam; 1:200) to detect macrophages, or rabbit polyclonal anti-phospho-p65 (Ser276, Santa Cruz Biotechnology; 1:100) to detect NF-κB pathway activation. FISH was performed using a probe for the conserved portion of prokaryotic 16S rRNA.

Morphometry

To quantify neutrophils and alveolar macrophages in alveolar tissue, these cells were identified by specific immunostaining, counted in 10 randomly non-overlapping tissue fields, and divided by the total number of alveoli present. Airway wall remodeling was evaluated by

measurement of subepithelial connective tissue volume density (VV_{airway}) according to published recommendations (27, 61). Only cross-sectional distal airways, covered predominantly by Club cells, were analyzed. Emphysematous changes of lung parenchyma were quantified using alveolar septal perimeter measurements and measurement of mean linear intercept on 10 randomly chosen fields of alveolar tissue at 200X magnification. All morphometric measurements were made using Image-Pro Express software (Media Cybernetics, Silver Springs, MD).

Immunodetection of IgA/NTHi binding

50 μL of a 0.2 mg/mL solution of NTHi (prepared as described above) was adsorbed onto a nitrocellulose membrane using a 96-well vacuum manifold. The membrane was washed twice with 0.1% PBS-Tween20 and then blocked for 30 minutes. After another two washes with 0.1% Tween20 in PBS (PBST), human SIgA from pooled colostrum (Sigma-Aldrich) was added and incubated for 1 hour. The membrane was again washed twice with 0.1% PBST, blocked for 30 minutes, and then incubated with rabbit polyclonal anti-IgA (Dako, Carpinteria, CA) to detect binding between NTHi and human IgA.

NF-κB measurement

Nuclear extracts were prepared from flash-frozen lung tissue using the NE-PER kit (Pierce, Rockford, IL). 10 μg of nuclear protein were separated on a 10% acrylamide gel. Western blot analysis was performed with antibodies against NF-κB p65 (Santa Cruz Biotechnology; 1:1000) or p84 (Genetex; 1:1000) with the Odyssey infared system (LI-COR).

MMP-12 and NE measurement

Whole tissue lysates were prepared from flash-frozen lung tissue using the c*O*mplete Lysis-M kit (Roche Diagnostics, Indianapolis, IN) and protein was separated on a 10% acrylamide gel. Western blot analysis was performed with Rabbit polyclonal antibodies against

MMP12 (#ab52897, Abcam; 1:1000), sheep polyclonal antibodies against neutrophil elastase (#61-86-20, Invitrogen, Camarille, CA; 1:1000) or rabbit polyclonal against β-actin (#A2066, Sigma-Aldrich, Saint Louis, MO; 1:2000).

Fluorescence imaging

Fluorescence imaging was performed according to a previously established protocol (120). Folate-PEG-Cy5 was purchased from Nanocs Inc., NY (excitation wavelength - 650 nm, emission - 670 nm). Animals were injected intravenously with 500 nmol/kg and fluorescent imaging was performed using a Pearl Impulse system (LI-COR, Lincoln, NE). Data were collected and analyzed using Pearl Impulse software (LI-COR).

16S rRNA quantification

Total prokaryotic burden was quantified using the Femto Bacterial DNA Quantification Kit (Zymo Research, Irvine, CA). Proprietary probes targeted the V1/V2 region of prokaryotic 16S rRNA. DNase/RNase-free water was used as a negative control.

Microbial community analysis

Lung tissue from 2 WT and 3 pIgR$^{-/-}$ mice was immediately flash frozen in liquid nitrogen after harvest. 25 mg of tissue from each mouse was homogenized and total genomic DNA extracted using the DNeasy Blood and Tissue Kit (Qiagen, Hilden, Germany). DNA was quantified and normalized to 2 ng/μl (Qubit 2.0 Fluorometer) prior to PCR amplification. Each sample was amplified in triplicate, parallel reactions with the universal 16S rRNA gene primers 27F (AGAGTTTGATCMTGGCTCAG) and 338R (GCTGCCTCCCGTAGGAGT) with barcoded adaptor sequences using NEBNext Master Mix (New England Biolabs, Ipswitch, MA). The amplicons were purified using Agencourt Ampure magnetic beads (Beckman-Coulter, Brea, CA) before being pooled. Sequencing was performed with paired end 250 bp reads on an Illumina

MiSeq at the Georgia Genomics Facility. The software package QIIME (121) was used for analysis of the microbial community dataset.

Chemokine measurements

KC levels were measured using Milliplex® magnetic beads according to the manufacturer's instructions with assistance from the Hormone Assay and Analytical Services Core of Vanderbilt University.

Statistical analysis

Mice were randomly assigned to the study groups and, where possible, researchers were blinded to the study groups until the time of statistical analysis. All animals were included in each analysis. Results are presented as mean ± standard deviation unless otherwise indicated. For experiments conducted over several time points or with multiple comparisons, a two-way ANOVA with a Bonferroni post-test was used. Pair-wise comparisons were made using Student's *t*-test. $p < 0.05$ was considered to be significant.

IV. AIRWAY BACTERIA DRIVE A PROGRESSIVE COPD-LIKE PHENOTYPE IN PIGR$^{-/-}$ MICE

This chapter was published in the journal *Nature Communications* (122).

Rationale

Chronic obstructive pulmonary disease (COPD) is a common smoking-related lung disease defined by fixed obstruction in expiratory airflow and characterized by chronic inflammation, fibrotic remodeling of small airways, and emphysematous destruction of lung parenchyma (123). Fibrotic narrowing of small airways occurs early in the course of COPD and, along with reduced elastic recoil, contributes to airflow obstruction (25, 27, 124). For many years, the predominant hypothesis regarding COPD pathogenesis has been that inhalation of toxic particles and gases, primarily from cigarette smoke, results in oxidant-mediated injury, airway inflammation, and disruption of the protease/anti-protease balance favoring lung parenchymal destruction (52, 125, 126). However, this theory does not fully explain the central role of small airways in this disease or continued airway inflammation and disease progression after smoking cessation (48, 49).

To protect the lungs from continuous exposure to inhaled irritants, particulates, and microorganisms, the airway epithelium forms tight junctions, supports an efficient mucociliary clearance apparatus, and maintains a thin airway surface liquid layer that contains a number of components with non-specific protective activity such as lactoferrin, lysozyme, and defensins (55, 65, 68). In addition, epithelial cells support an antigen-specific secretory IgA (SIgA) barrier that covers and protects the airway surface (71, 72, 84). In small airways, polymeric IgA (pIgA) is produced by sub-epithelial plasma cells and transported from the basolateral to apical surface of epithelial cells through binding to the polymeric immunoglobulin receptor (pIgR).(69, 127) At the apical surface, pIgR is cleaved to release the secretory component of pIgR joined to pIgA (together forming SIgA) into the airway surface liquid. Through a process known as immune exclusion, SIgA agglutinates airborne antigens and microorganisms, preventing them from

activating or injuring airway epithelial cells (72-74). In patients with COPD, widespread structural abnormalities of the airway epithelium are common and correlate with decreased expression of pIgR and disruption of the SIgA barrier in individual airways (61, 65, 85, 87, 128). We have shown that the level of SIgA on the luminal surface of individual small airways correlates inversely with the degree of airway wall remodeling in COPD patients and mean SIgA levels in all small airways across a section of excised lung predicts severity of airflow obstruction (61). In addition, reduced levels of SIgA are present in bronchoalveolar lavage (BAL) from patients with severe COPD (61, 88). To date, however, the contribution of SIgA deficiency to COPD pathogenesis has not been determined. Therefore, we studied mice with genetic deletion of pIgR, which cannot form SIgA on mucosal surfaces. Our studies indicate that pIgR$^{-/-}$ mice develop progressive COPD-like airway and parenchymal remodeling as they age that result from persistent activation of inflammatory signaling by the lung microbiota, thus pointing to a causative role for SIgA deficiency in persistent inflammation and disease progression in COPD.

Results

LUNG INFLAMMATION AND REMODELING IN PIGR$^{-/-}$ MICE

We obtained pIgR$^{-/-}$ mice (C57BL/6 background) (119, 129) and performed immunofluorescence microscopy to show that SIgA was not detectable on the airway surface (**Figure 4A-B**). Although pIgR$^{-/-}$ mice appeared healthy at birth and demonstrated no histopathologic changes in the lungs compared to wild-type (WT) littermate controls at 2 months of age, pIgR$^{-/-}$ mice developed COPD-like changes with fibrotic small airway remodeling and emphysematous destruction of the lung parenchyma by 6 months of age that continued to worsen in 12 month-old mice (**Figure 5A, C-E)**. Despite the presence of airway wall remodeling in pIgR$^{-/-}$ mice, airway epithelial structure appeared intact without evidence of goblet cell hyperplasia or stratification. Similar to COPD patients, (130, 131) aging pIgR$^{-/-}$ mice displayed

fragmentation and degradation of the elastin network in alveolar walls and around small airways (**Figure 5B**). Importantly, unlike other genetic models of COPD, (43) the lack of COPD-like changes in 2 month-old (young adult) pIgR$^{-/-}$ mice indicates that this phenotype is not related to developmental defects resulting from in utero pIgR deficiency.

After identifying COPD-like changes in the lungs of pIgR$^{-/-}$ mice, we quantified inflammatory cells in the lungs. At 2 months of age, WT and pIgR$^{-/-}$ mice showed similar numbers of neutrophils and macrophages in lung parenchyma and in BAL; however, by 6 and 12 months of age, pIgR$^{-/-}$ mice had a marked increase in inflammatory cells compared to 2 month-old mice and to age-matched WT controls (**Figure 6A-E)**. Macrophage accumulation in the lungs of pIgR$^{-/-}$ mice was similar at 6 and 12 months of age, but the neutrophil influx continued to increase between 6 and 12 months of age. In addition, lymphocytes were found to be increased in lungs of pIgR$^{-/-}$ mice compared to WT controls. Total lymphocyte counts in BAL were 789±135 in 12 month-old WT mice compared to 3027±287 in 12 month-old pIgR$^{-/-}$ mice ($p<0.001$).

We recently developed a non-invasive *in vivo* molecular imaging technique that utilizes a fluorescent probe (folate-PEG-Cy5) to identify activated macrophages based on expression of folate receptor beta (FRβ).(120) As shown in **Figure 7A-B**, increased fluorescent signal was detected over the lungs of 12 month-old pIgR$^{-/-}$ mice compared to age-matched WT controls, indicating an increase in activated macrophages in the lungs of these mice. Interestingly, we observed no difference in the fluorescent signal over the abdomen of pIgR$^{-/-}$ mice, suggesting that increased macrophage activation was limited to lungs.

Activated macrophages and neutrophils can produce matrix metalloproteinase (MMP)-12 and neutrophil-derived elastase (NE) respectively, which have been linked to emphysematous remodeling (132-135). Therefore, we measured MMP-12 and NE in lung homogenates and found significantly increased levels of both these enzymes in 12 month-old pIgR$^{-/-}$ mice compared to age-matched WT mice (**Figure 7C**). Together, these data indicate that pIgR$^{-/-}$ mice

develop a persistent inflammatory and destructive environment in the lungs as they age, likely contributing to the COPD phenotype observed in these mice.

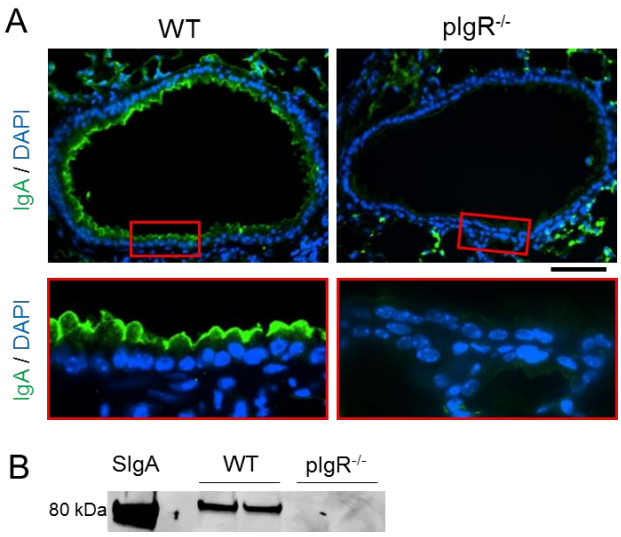

Figure 4: pIgR$^{-/-}$ mice lack SIgA in small airways.

A) Immunofluorescence staining for IgA (green) showing SIgA on the epithelial surface of a small airway from a wild-type (WT) mouse and no detectable SIgA on the airway surface of a pIgR$^{-/-}$ mouse (200X; insets 1000X). Scale bar = 50 μm. **B**) Western blot for secretory component in bronchoalveolar lavage fluid from WT and pIgR$^{-/-}$ mice. SIgA from human colostrum was used as a positive control.

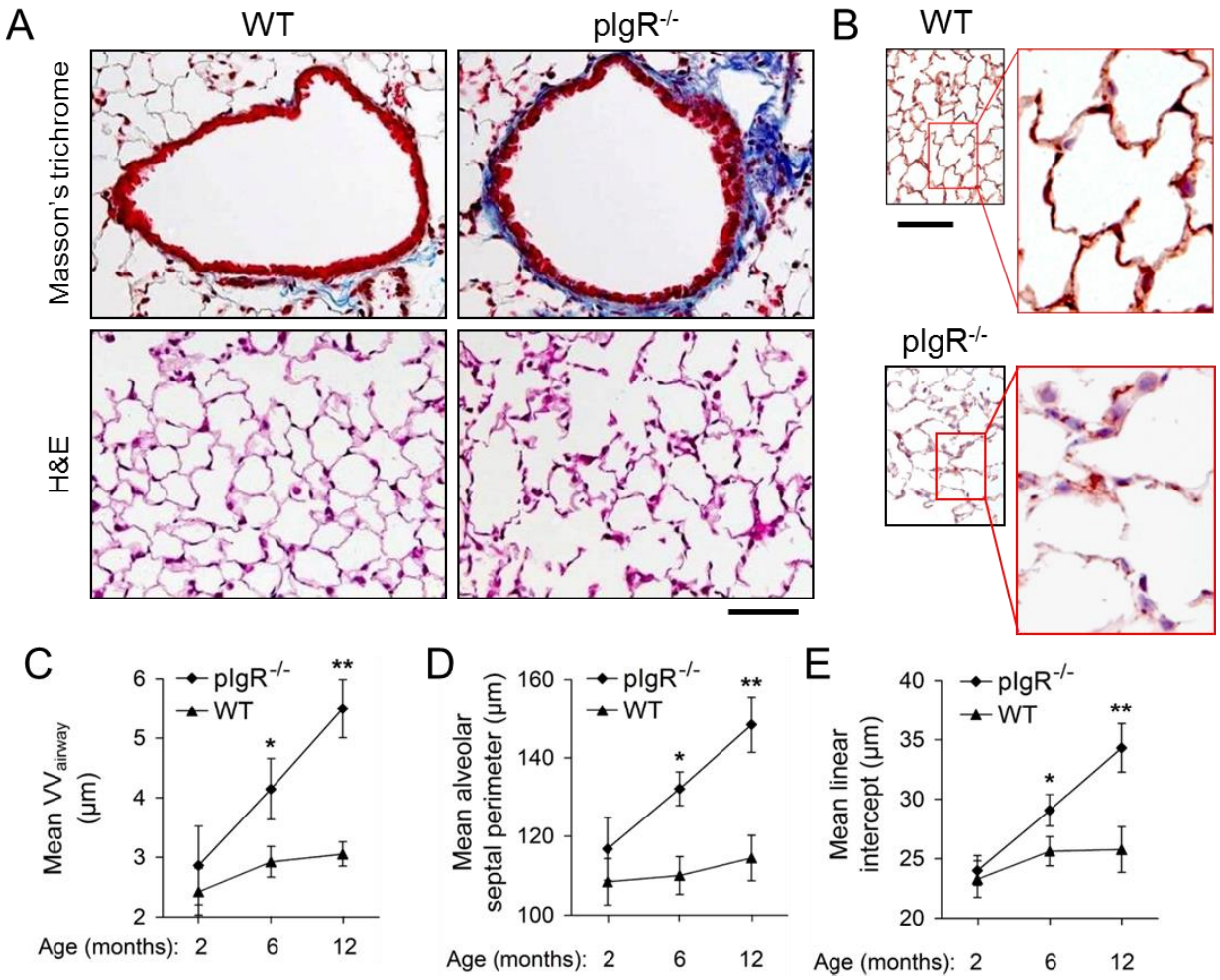

Figure 5: pIgR$^{-/-}$ mice develop progressive COPD-like small airway and parenchymal remodeling.

A) Representative images of small airway remodeling (Masson's trichrome, 200X) and emphysema (H&E, 200X) in a 12 month-old pIgR$^{-/-}$ mouse compared to a WT control. Scale bar = 50 μm. **B**) Immunostaining for elastin in 12 month-old WT and pIgR$^{-/-}$ mouse shows reduction and fragmentation of elastin in inter-alveolar septa in a pIgR$^{-/-}$ mouse compared to the intact elastin network in WT mouse (100X; insets 1000X). **C-E**) Morphometric analysis showing increased wall thickness (VV_{airway}), mean alveolar septal perimeter length, and mean linear intercept in pIgR$^{-/-}$ and age-matched WT littermate controls at the indicated ages. Five-10 mice per group; * = $p<0.01$ compared to 2 month-old pIgR$^{-/-}$ mice and age-matched WT controls, ** = $p<0.001$ compared to all other groups (two-way ANOVA).

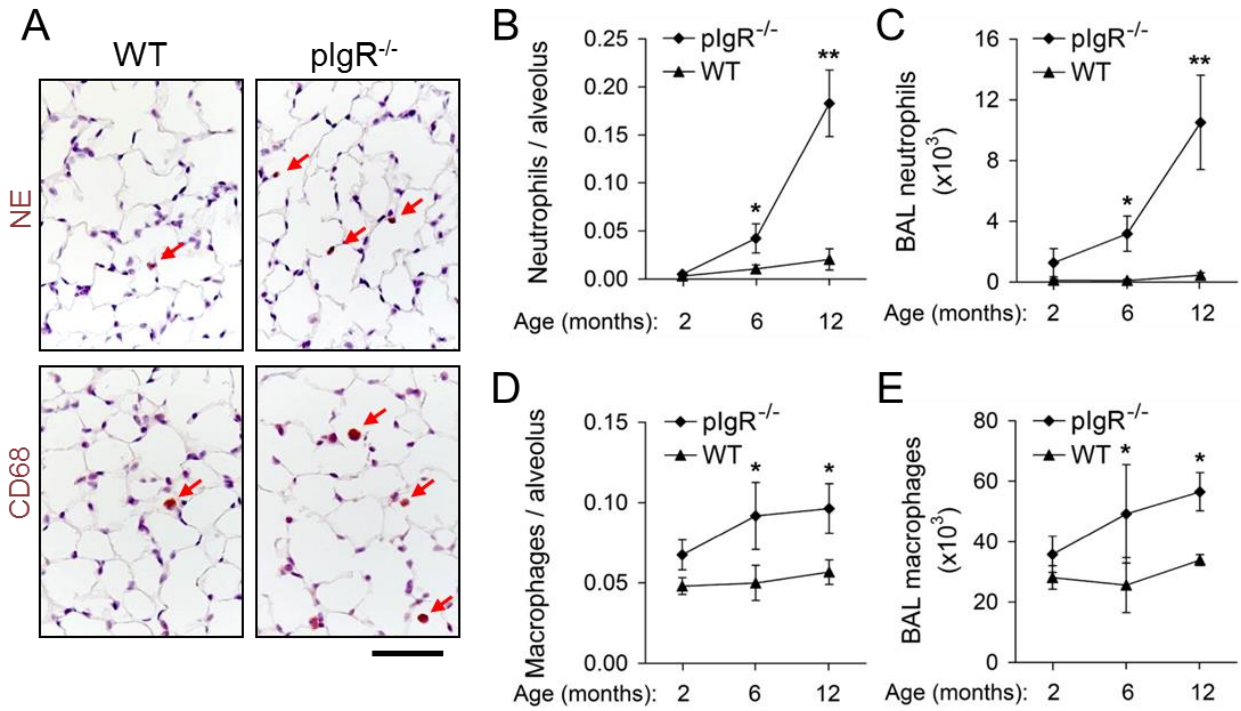

Figure 6: pIgR$^{-/-}$ mice develop progressive airway and parenchymal inflammation.

A) Representative immunostains for neutrophils using antibodies to neutrophil elastase (NE) or macrophages using antibodies to CD68 in 12 month-old WT and pIgR$^{-/-}$ mice. Positive cells are stained brown (indicated by red arrows) (200X). Scale bar = 50 μm. **B-E**) Neutrophil (NE+) and macrophage (CD68+) counts in lungs of pIgR$^{-/-}$ and age-matched WT littermate controls at the indicated ages and neutrophil and macrophage counts in BAL fluid. Five-7 mice per group; * = $p<0.05$ compared to 2 month-old pIgR$^{-/-}$ mice and age-matched WT mice; ** = $p<0.01$ compared to all other groups (two-way ANOVA).

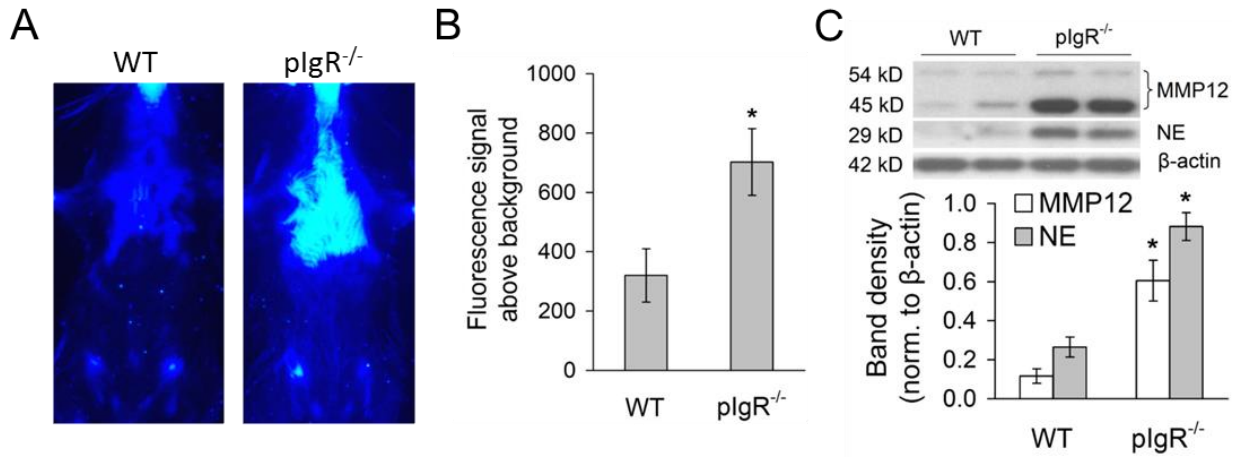

Figure 7: Macrophage and neutrophil activation in pIgR$^{-/-}$ mice.

A) Representative image of folate-PEG-Cy5-derived chest fluorescence 4 hours after IV probe injection in 12 month-old WT and pIgR$^{-/-}$ mice. **B**) Photon emission from the chest normalized to background prior to injection of probe. Three-4 mice per group; * = $p<0.05$ (Student's *t*-test). **C**) Western blot and densitometry for MMP-12 (two bands at 45 and 54 kDa) and NE (29 kDa) in lung tissue from 12 month-old WT and pIgR$^{-/-}$ mice. Band densities of MMP-12 and NE were normalized to β-actin. Six mice per group; * = $p<0.01$ compared to WT mice (Student's *t*-test).

BACTERIAL INVASION AND NF-κB ACTIVATION IN PIGR$^{-/-}$ MICE

Since loss of mucosal immunity in pIgR$^{-/-}$ mice results in chronic inflammation in the lungs, we wondered whether lack of SIgA could render small airways more susceptible to invasion by airway bacteria with subsequent activation of inflammatory signaling in epithelial cells. Therefore, we performed fluorescent *in situ* hybridization (FISH) on lung sections from WT and pIgR$^{-/-}$ mice using probes specific for the conserved portion of the bacterial gene encoding 16S ribosomal RNA (16S rRNA) (**Figure 8A, top panels**). While a significant proportion of airways in pIgR$^{-/-}$ mice showed bacteria localized within the airway epithelium (between the apical epithelial border and basement membrane), this was almost never observed in WT airways. In contrast, the percentage of airways with bacteria present in the airway lumen did not differ between WT and pIgR$^{-/-}$ mice (**Figure 8B**). These findings suggest that an impaired mucosal immune barrier in pIgR$^{-/-}$ mice allows migration of colonizing airway bacteria across the apical epithelial border.

Bacteria can initiate innate immune signaling in the epithelium through activation of Toll-like receptors, leading to activation of the NF-κB pathway. To investigate whether this pathway was activated in pIgR$^{-/-}$ mice, we performed fluorescent immunostaining for an activated form of the p65(RelA) component of NF-κB (phosphoserine 276)(136-138) (**Figure 8A, bottom panels**). While detection of phospho-p65 (Ser276) staining in nuclei of airway epithelial cells was rare in WT mice, a marked up-regulation of phospho-p65 was detected in lungs of 6 and 12 month-old pIgR$^{-/-}$ mice. We also evaluated NF-κB activation in lung tissue by western blot and found increased p65 in nuclear protein extracts from pIgR$^{-/-}$ mice compared to age-matched WT controls, further supporting increased NF-κB activation in these mice (**Figure 8C**). In addition, we identified a significant increase in the concentration of the NF-κB dependent chemokine KC in BAL fluid from pIgR$^{-/-}$ mice compared to age-matched WT mice (**Figure 8D**). The combination of bacterial localization within the airway epithelium and increased epithelial NF-κB

activation in pIgR$^{-/-}$ mice supports the conclusion that loss of surface SIgA allows colonizing bacteria to penetrate the epithelial barrier and activate inflammatory signaling.

To determine whether pIgR deficiency alters the density or composition of the lung microbiome, we analyzed bacterial abundance and taxonomy in the lungs of age-matched WT and pIgR$^{-/-}$ mice. First, we measured total bacterial DNA by qPCR targeting the V1/V2 portion of bacterial 16s rRNA in 9 month-old mice and found no difference in total bacterial burden in the lungs of WT and pIgR$^{-/-}$ mice (**Figure 8E**). Subsequently, we used high throughput amplicon sequencing to evaluate microbial communities in whole lung tissue from 6 month-old WT and pIgR$^{-/-}$ mice. As has been reported previously (139), Proteobacteria and Firmicutes were the most common bacterial phyla present in the lungs of both groups of mice (**Figure 9**). Compared to WT mice, pIgR$^{-/-}$ mice had a two-fold increase (400 vs. 194) in the number of detected operational taxonomic units (OTUs). Analysis by Random Forests, a supervised machine learning technique, was used to classify microbial taxa that discriminate the mouse genotypes (140). Ten OTUs that best discriminate the genotypes are shown in **Figure 10**.

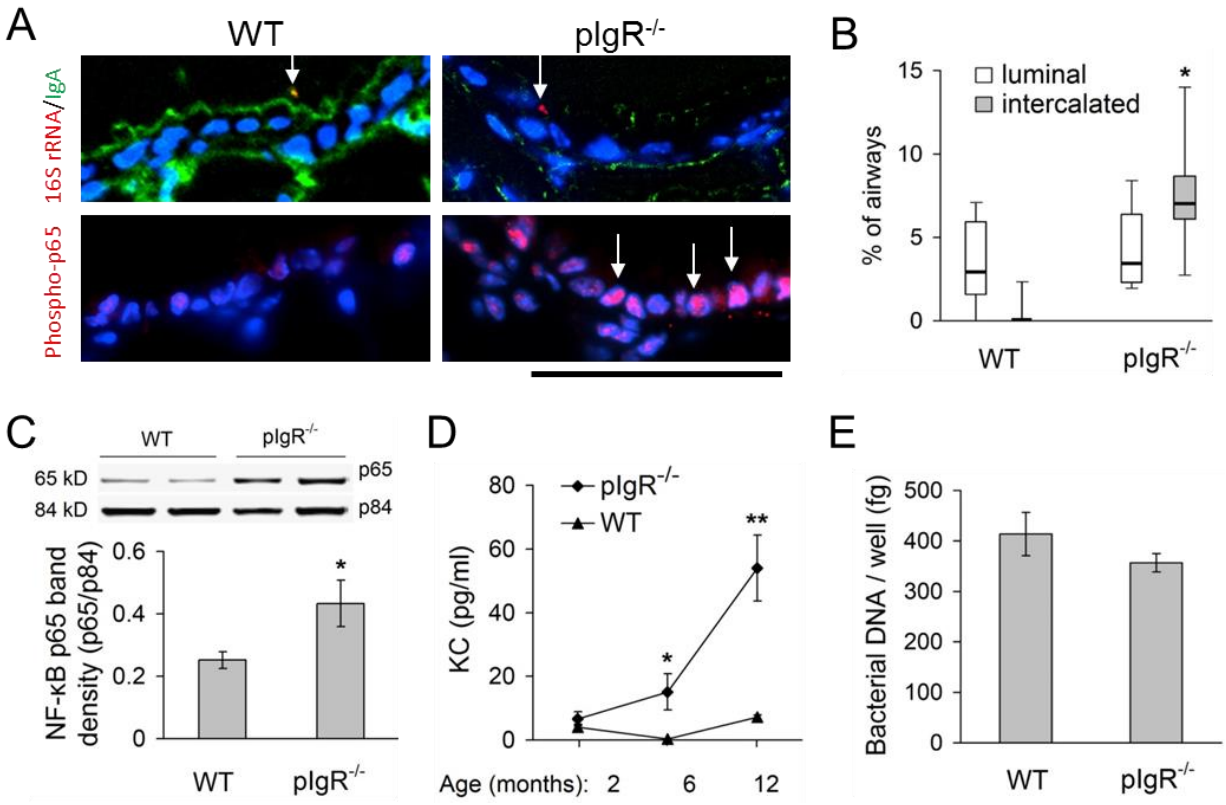

Figure 8: Bacterial invasion and NF-κB activation in the lungs of pIgR$^{-/-}$ mice.

A) Immunofluorescent detection of bacteria (FISH probe for 16S rRNA, red, top panels) or NF-κB [phospho-p65 (Ser276, red, bottom panels], IgA (green, top panels), and DAPI (blue) from 12 month-old WT and pIgR$^{-/-}$ mice (1000X). In WT mice, bacteria with bound SIgA were identified within the airway lumen (yellow on merged image, identified by arrow), whereas bacteria intercalated within the epithelium were identified in pIgR$^{-/-}$ mice (red, identified by arrow). Bottom panels show phopsho-p65 localized to nuclei (arrows). Scale bar = 50 μm. **B**) Box and whisker plot (showing median, 25th-75th percentile, and range) for intraepithelial (intercalated) and luminal bacteria in airways of 12 month-old WT and pIgR$^{-/-}$ mice as identified by FISH for bacterial DNA. Seven mice per group; * = p<0.001. **C**) Western blot and densitometry for p65 component of NF-κB (normalized to p84) in nuclear protein extracts from lungs of 12 month-old WT and pIgR$^{-/-}$ mice. Six mice per group; * = p<0.05 (Student's *t*-test). **D**) KC protein levels in BAL fluid. Six mice per group; * = p<0.05 compared to 2 month-old pIgR$^{-/-}$ mice and age-matched WT controls; ** = p<0.05 compared to all other groups (two-way ANOVA). **E**) Total bacterial DNA was quantified from lung tissue in WT and pIgR$^{-/-}$ mice using qPCR and primers specific for V1 region of prokaryotic 16s rRNA. Ten mice per group.

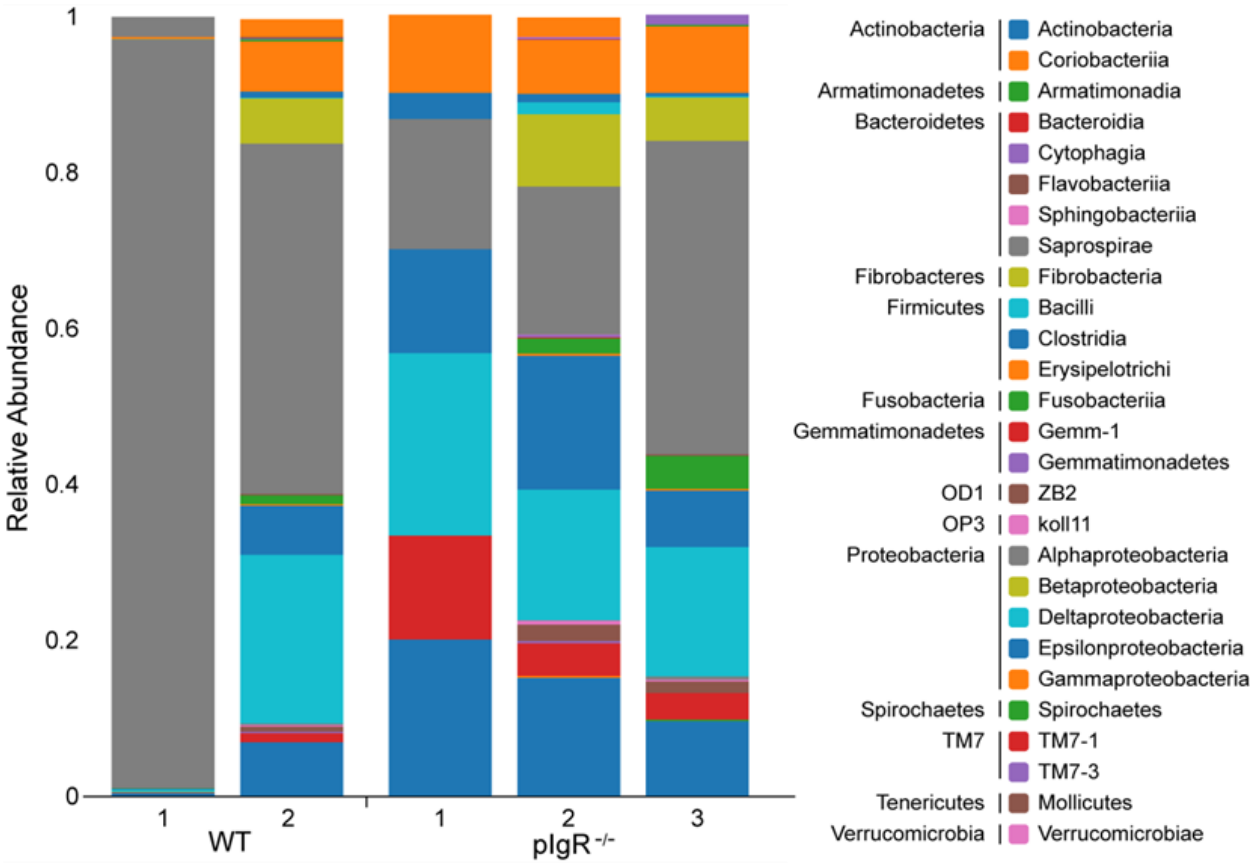

Figure 9: Distribution of bacterial phyla and classes in lung tissue in WT and pIgR$^{-/-}$ mice.

Distribution of bacterial phyla and classes in lung tissue as determined by 16S sequencing from lungs of individual 12 month-old WT and pIgR$^{-/-}$ mice.

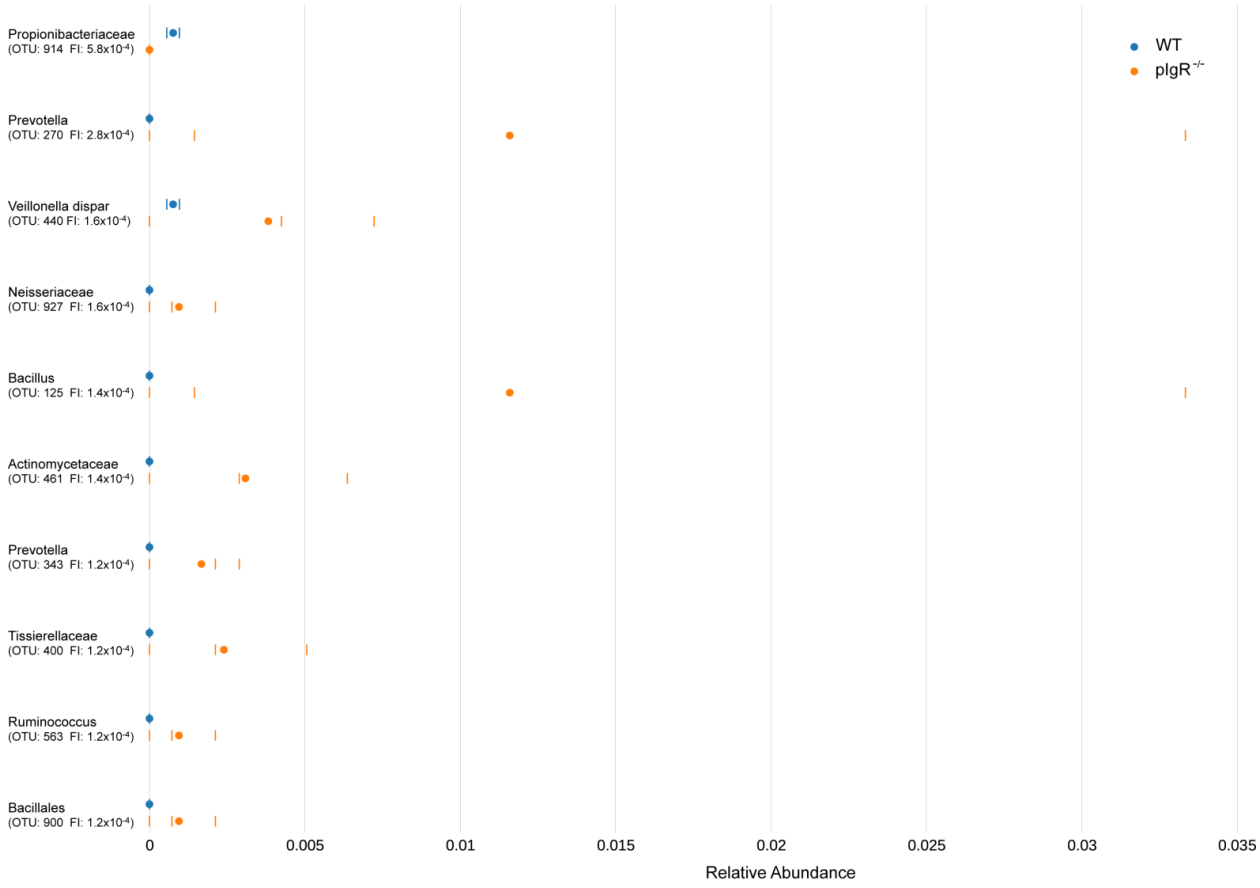

Figure 10: Average abundance of OTUs with feature importance by genotype.

Average abundance of OTUs (circle) as ranked according to random forest analysis of important features (FI) in treatment analysis of all sequences (error rate = 0.75% ± 0.5% SD). Abundance of OTUs in individual samples are represented as the tick mark. WT mice are shown in blue and pIgR$^{-/-}$ mice are shown in orange.

SIgA MODULATES THE ACUTE INFLAMMATORY RESPONSE TO NTHi

To investigate whether pIgR deficiency directly alters the inflammatory response to bacterial products, we treated 2 month-old WT or pIgR$^{-/-}$ mice with lysates prepared from non-typeable *Haemophilus influenzae* (NTHi). Although NTHi is not a mouse pathogen, NTHi was selected for study because it is the most common bacterium identified in the respiratory tract of patients with COPD both during disease exacerbations and stable periods (141, 142). Compared to WT mice, pIgR$^{-/-}$ mice treated with aerosolized NTHi lysate had increased inflammation as determined by neutrophil influx after 24 hours (**Figure 11A-B**). To determine whether exogenous SIgA could mitigate inflammation induced by NTHi lysates, we obtained SIgA from pooled human colostrum, showed that this SIgA binds to proteins in NTHi lysates, and delivered SIgA into the lungs of pIgR$^{-/-}$ mice by intratracheal (IT) injection (**Figure 11C-D**). At 24 hours after exposure to aerosolized NTHi lysates, pIgR$^{-/-}$ mice treated with IT SIgA showed a marked reduction in NTHi-induced lung inflammation and NF-κB activation compared to pIgR$^{-/-}$ mice treated with vehicle (**Figure 11E-G**), indicating that the presence of SIgA limits the inflammatory response to bacterial antigens in the lungs.

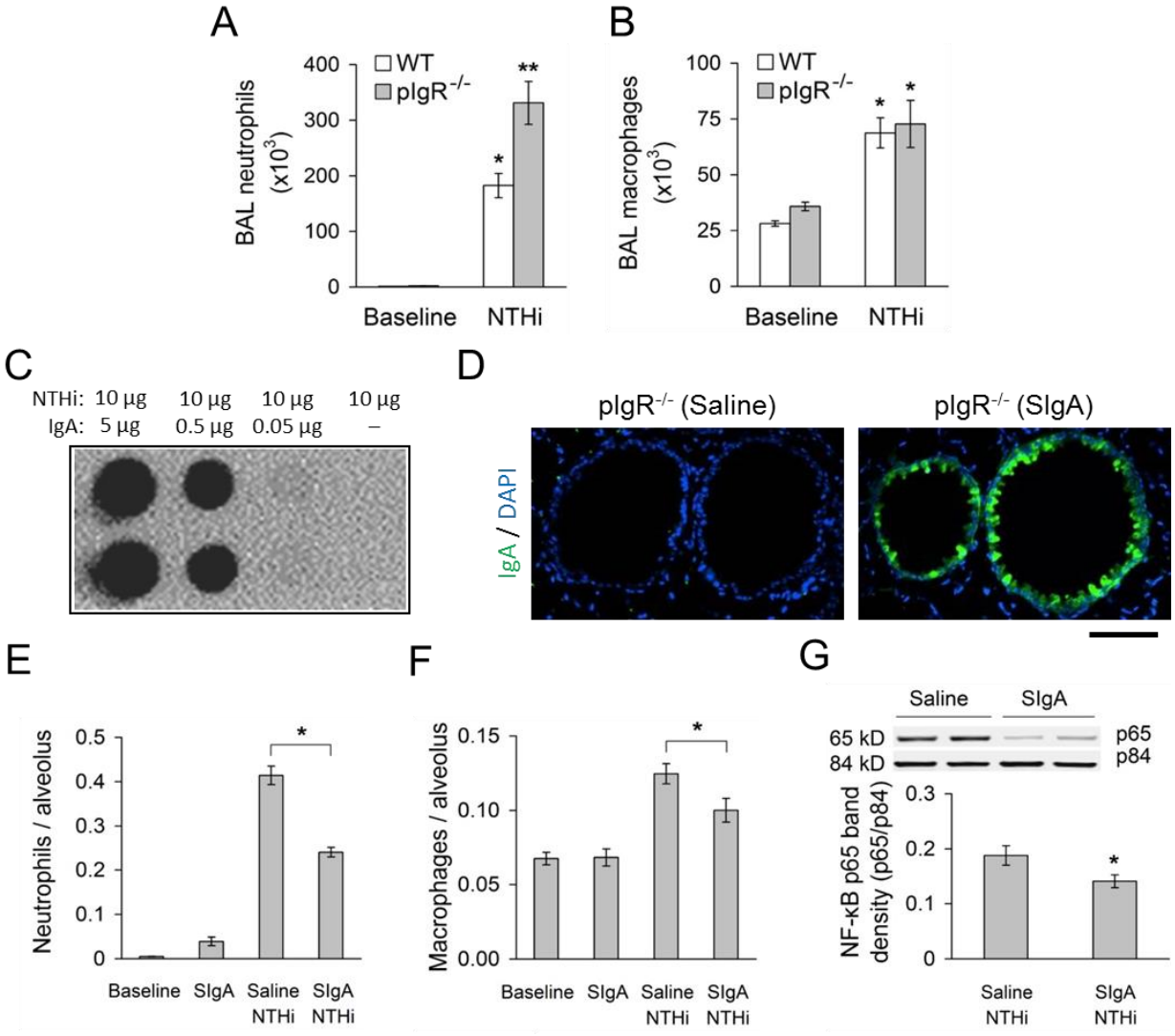

Figure 11: SIgA modulates the acute inflammatory response to NTHi *in vivo*.

A,B) Neutrophil and macrophage counts in BAL fluid from 2 month-old WT and pIgR$^{-/-}$ mice 24 hours after aerosolization of non-typeable *Haemophilus influenzae* (NTHi) lysate (10 mg). Six-8 mice per group; * = p<0.01 compared to untreated mice (baseline), ** = p<0.01 compared to WT mice treated with NTHi (Student's *t*-test). **C**) Dot-blot assay demonstrating protein binding between NTHi lysates and human SIgA from colostrum. **D**) Immunofluorescent detection of human SIgA (green) in the lungs of pIgR$^{-/-}$ mouse 1 hour after intratracheal delivery of SIgA or vehicle (normal saline) (200X). Scale bar = 50 µm. **E,F**) Parenchymal neutrophil and macrophage counts 24 hours after aerosol delivery of NTHi lysate to 2 month-old pIgR$^{-/-}$ mice pretreated with intratracheal SIgA (50 µL of 0.34 mg/mL solution) or vehicle (normal saline). Macrophage and neutrophil numbers were quantified by immunostaining for CD68 or NE, respectively. Five-6 mice per group; * = p<0.05 compared to mice pretreated with saline followed by NTHi (Student's *t*-test). (**g**) Western blot and densitometry for p65 component of NF-κB (normalized to p84) in lung nuclear protein extracts from 2 month-old pIgR$^{-/-}$ mice pretreated with intratracheal SIgA or normal saline 1 hour prior to NTHi nebulization and harvested 24 hours later. Six mice per group; * = p<0.05 (Student's *t*-test).

BACTERIA DRIVE THE COPD-LIKE PHENOTYPE IN PIGR$^{-/-}$ MICE

Given our observation that pIgR$^{-/-}$ mice have increased bacterial invasion across the mucosal surface of the airways, changes in microbial composition, and a heightened inflammatory response, we postulated that endogenous bacterial flora in pIgR$^{-/-}$ mice could be responsible for driving persistent inflammation and COPD-like remodeling in the lungs of these mice. To test this concept, germ-free pIgR$^{-/-}$ and WT mice (C57BL/6 background) were generated at the National Gnotobiotic Rodent Resource Center (University of North Carolina at Chapel Hill) and maintained in sterile conditions. In contrast to pIgR$^{-/-}$ mice maintained in standard housing, 6 month-old germ-free pIgR$^{-/-}$ mice were completely protected from small airway remodeling and emphysema (**Figure 12A-E)**. While the COPD-like remodeling progressed from 6-12 months of age in pIgR$^{-/-}$ mice housed in standard conditions, no evidence of small airway remodeling or emphysema was observed in germ-free pIgR$^{-/-}$ mice, even at 12 months of age. Neutrophils were essentially undetectable in the alveolar parenchyma from germ-free pIgR$^{-/-}$ and WT mice and macrophage counts in germ-free pIgR$^{-/-}$ mice were reduced to levels similar to WT mice (with standard or sterile housing) (**Figure 12F-G**). To investigate the impact of reconstituting the microbiome in adult pIgR$^{-/-}$ mice, we removed a cohort of mice from germ-free conditions at 6 months of age and housed them in standard conditions for 6 months. As shown in **Figure 12C-G**, 12 month-old pIgR$^{-/-}$ mice (which were maintained in standard housing for 6 months) demonstrated similar levels of airway wall remodeling, emphysema, and inflammation to 6 month-old pIgR$^{-/-}$ mice raised in standard housing. Cumulatively, these results implicate airway bacteria as the primary driver of inflammation and COPD-like histopathologic changes in pIgR$^{-/-}$ mice.

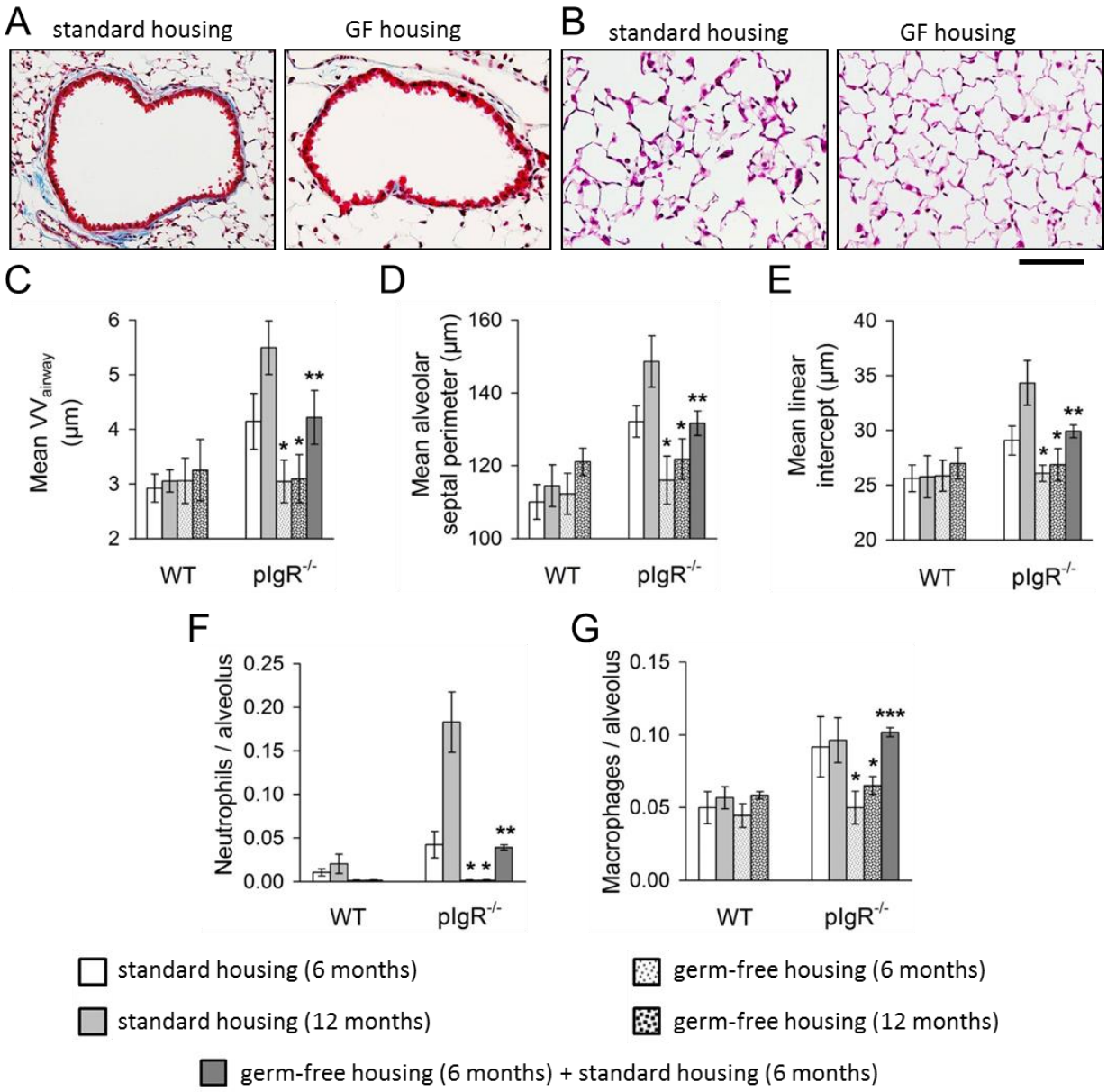

Figure 12: Germ-free pIgR$^{-/-}$ are protected from COPD-like lung remodeling.

A) Representative images of small airway remodeling (Masson's trichrome, 200X) and emphysema **B**) (H&E, 200X) in a 6 month-old pIgR$^{-/-}$ mouse in standard housing compared to a 6 month-old pIgR$^{-/-}$ mouse housed in germ-free conditions. Scale bar = 50 µm. **C-E**) Morphometric analysis of airway wall thickness (VV_{airway}), alveolar septal perimeter length, and mean linear intercept in 6 and 12 month-old WT and pIgR$^{-/-}$ mice maintained in standard housing, germ-free housing, or 6 months of germ-free housing followed by 6 months of standard housing as indicated. **F,G**) Parenchymal neutrophil (NE+) and macrophage (CD68+) counts in lungs of 6 and 12 month-old WT and pIgR$^{-/-}$ mice maintained in standard housing, germ-free housing, or combination as indicated. Six-7 mice per group; * = p<0.001 compared to all other groups, ** = p<0.001 compared to age-matched WT controls housed in standard conditions (two-way ANOVA).

ROFLUMILAST BLOCKS COPD PROGRESSION IN PIGR$^{-/-}$ MICE

Next, to investigate whether progressive small airway remodeling and emphysema in pIgR$^{-/-}$ mice occur in response to bacteria-induced inflammation, we utilized the anti-inflammatory drug roflumilast, which inhibits phosphodiesterase-4. Roflumilast is FDA-approved for use in COPD patients and has been shown to reduce inflammation in murine models of COPD (143-146). For these studies, 9 month-old WT or pIgR$^{-/-}$ mice were treated daily by oral gavage with 100 µg of roflumilast (5 µg/g) or vehicle (4% methylcellulose, 1.3% PEG400) for 3 months and lungs were harvested at 12 months of age. Unlike pIgR$^{-/-}$ mice treated with vehicle, mice treated with roflumilast had no progression of small airway wall remodeling after starting treatment (**Figure 13A**). Strikingly, 12 month-old pIgR$^{-/-}$ mice treated with roflumilast had reduced indices of emphysema compared to 9 month-old pIgR$^{-/-}$ mice, indicating that roflumilast not only blocks progression of emphysema in this model but apparently facilitates some resolution of the emphysematous destruction of lung parenchyma (**Figure 13B-C**). Similar to mice housed in germ-free conditions, WT and pIgR$^{-/-}$ mice treated with roflumilast had very few neutrophils in the lung parenchyma (**Figure 14A**) and macrophage numbers were equivalent to vehicle-treated WT mice (**Figure 14B**). Consistent with decreased inflammation, roflumilast treatment resulted in reduced MMP-12 and NE in lungs of pIgR$^{-/-}$ mice (**Figure 14B**). In addition, NF-κB activation and KC expression were reduced in lungs of roflumilast-treated pIgR$^{-/-}$ mice compared with vehicle-treated pIgR$^{-/-}$ mice (**Figure 14D-E**). Together, these data indicate that persistent bacterial-derived inflammation propels COPD-like remodeling in pIgR$^{-/-}$ mice.

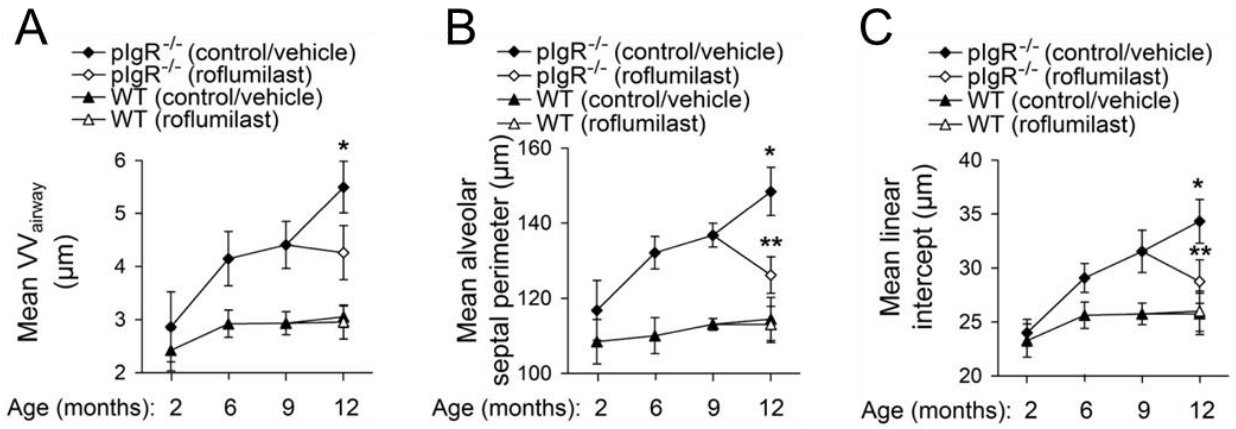

Figure 13: Roflumilast blocks COPD-like lung remodeling in pIgR$^{-/-}$ mice.

A-C) Morphometric analysis showing small airway wall thickness (VV_{airway}), mean alveolar septal perimeter length, and mean linear intercept at the indicated ages in pIgR$^{-/-}$ and WT mice treated with roflumilast or vehicle from 9-12 months of age. 5-10 mice per group; * = $p<0.01$ compared to 12 month-old pIgR$^{-/-}$ mice treated with roflumilast, ** = $p<0.05$ compared to 6 and 9 month-old pIgR$^{-/-}$ mice (two-way ANOVA).

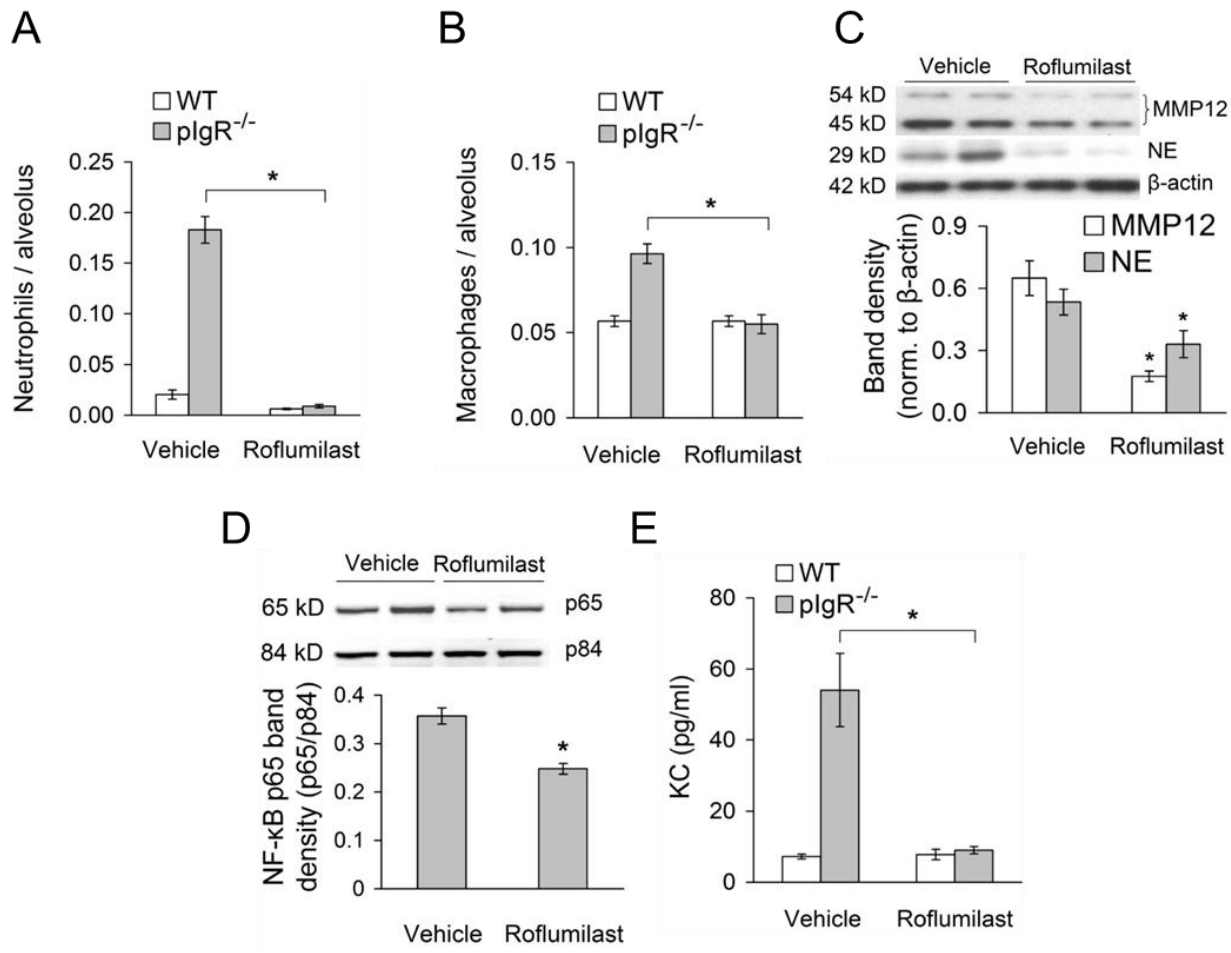

Figure 14: Roflumilast blocks lung inflammation in pIgR$^{-/-}$ mice.

A,B) Parenchymal neutrophil and macrophage counts in 12 month-old WT and pIgR$^{-/-}$ mice treated for 3 months with roflumilast or vehicle. Six-7 mice per group; * = p<0.01 (macrophages) or p<0.001 (neutrophils) compared to pIgR$^{-/-}$ mice treated with vehicle (Student's *t*-test). **C**) Western blot and densitometry for MMP-12 and NE in lung tissue from 12 month-old pIgR$^{-/-}$ mice treated with roflumilast or vehicle. Band densities of MMP-12 and NE were normalized to β-actin. 6 mice per group; * = p<0.05 (Student's *t*-test). **D**) Western blot and densitometry for p65 component of NF-κB (normalized to p84) in lung nuclear protein extracts from 12 month-old pIgR$^{-/-}$ mice treated with roflumilast or vehicle. 6 mice per group; * = p<0.01 (Student's *t*-test). **E**) KC protein levels in BAL fluid from 12 month-old WT or pIgR$^{-/-}$ treated with roflumilast or vehicle. 6 mice per group; * = p<0.05 compared to pIgR$^{-/-}$ mice treated with vehicle (Student's *t*-test).

EFFECTS OF CIGARETTE SMOKE IN PIGR$^{-/-}$ MICE

To determine how spontaneous COPD-like remodeling in pIgR$^{-/-}$ mice compares to long-term cigarette smoke (CS) exposure, we treated 2 month-old WT and pIgR$^{-/-}$ mice with mainstream CS twice daily for 6 months according to a protocol previously shown to induce emphysema (147). WT mice treated with CS developed a similar degree of small airway wall remodeling and emphysema compared to sham-treated pIgR$^{-/-}$ mice; however, CS exposure worsened COPD-like remodeling in pIgR$^{-/-}$ mice (**Figure 15A-D**). No evidence of structural airway epithelial changes, including goblet cell hyperplasia or stratification, or development of lymphoid aggregates or tertiary lymphoid follicles, was present in any group of mice (with or without CS treatment). Compared to age-matched, sham-treated WT controls, increased inflammatory cells (neutrophils and macrophages) were observed in CS-treated WT mice and pIgR$^{-/-}$ mice with or without CS treatment (**Figure 15E-F**). The only observed difference between CS-treated WT mice and sham-treated pIgR$^{-/-}$ mice was a mild increase in neutrophil influx in the CS-treated WT group. In this study, the highest degree of remodeling and inflammation was present in CS-treated pIgR$^{-/-}$ mice, indicating an additive effect between pIgR$^{-/-}$ deficiency and CS exposure in this model.

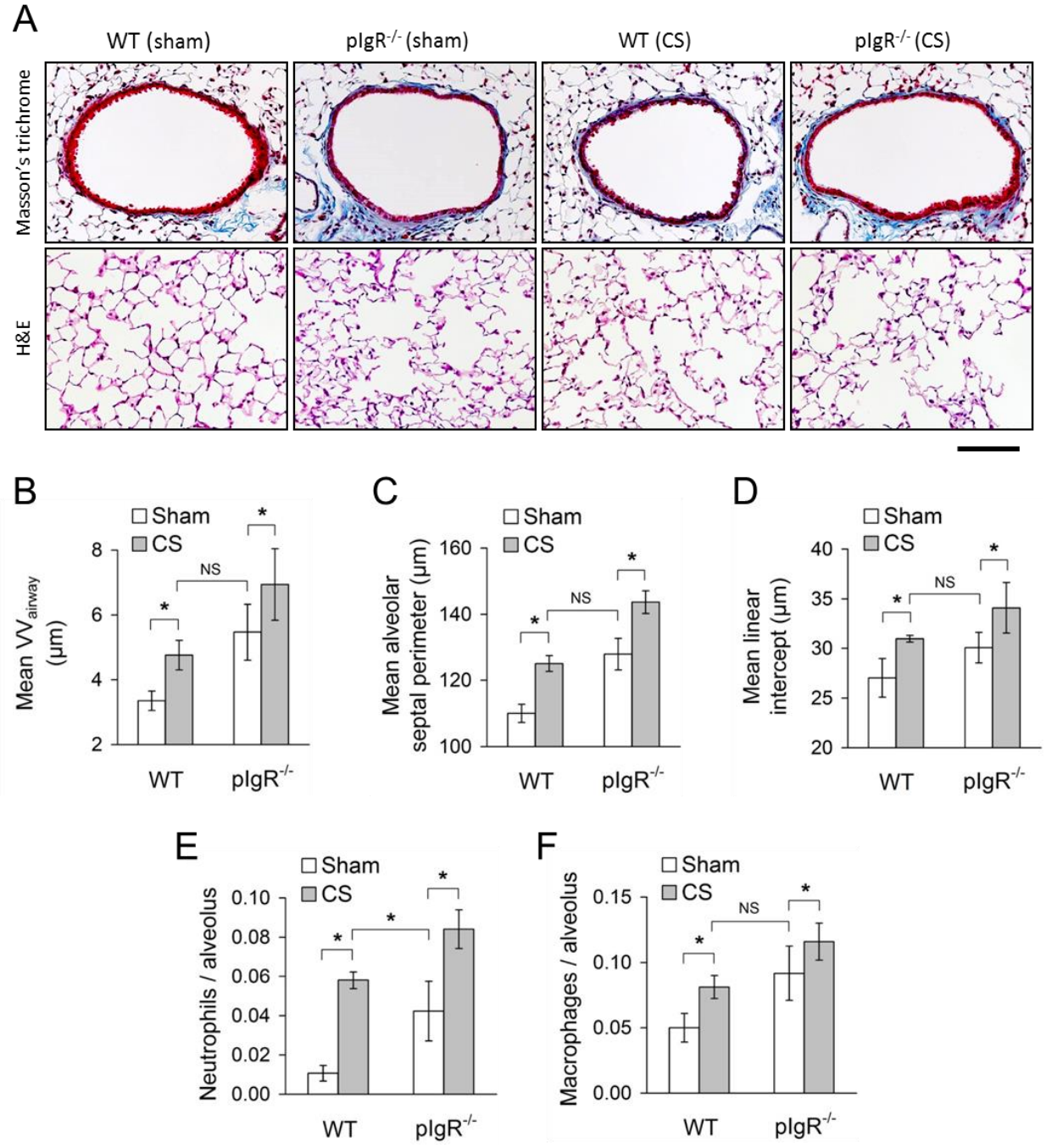

Figure 15: Cigarette smoke increases airway remodeling and emphysema in pIgR$^{-/-}$ mice.

A) Representative images of small airway remodeling (Masson's trichrome, 200X) and emphysema (H&E, 200X) in WT and pIgR$^{-/-}$ mice treated twice daily with mainstream cigarette smoke or sham control (filtered air) for 6 months (between 2 and 8 months of age). Scale bar = 50 μm. **B-D**) Morphometric analysis of small airway wall thickness (VV_{airway}), mean alveolar septal perimeter length, and mean linear intercept length. Five mice per group; * = p<0.01 compared to WT mice treated with sham; ** = p<0.01 compared to all other groups (two-way ANOVA). **E,F**) Parenchymal neutrophil and macrophage counts in lung tissue from WT or pIgR$^{-/-}$ mice. Five mice per group; * = p<0.01 compared to WT mice treated with sham; ** = p<0.01 compared to all other groups (two-way ANOVA).

Discussion

This work elucidates an important role for the SIgA immune system in maintaining homeostasis in the lungs by showing that disruption of this first line of mucosal host defense leads to persistent activation of innate immunity, which is normally reserved as a second line of host defense. Chronic innate immune activation, in turn, drives tissue injury and progressive lung remodeling. Mice with a defective SIgA immune system in the lungs due to pIgR deficiency develop a pattern of small airway and parenchymal remodeling that recapitulates pathological changes seen in human COPD. This phenotype worsens with aging, indicating that injury and remodeling due to pIgR/SIgA deficiency are additive and progressive. $pIgR^{-/-}$ mice develop increased bacterial invasion into small airway walls, resulting in epithelial cell NF-κB activation, leukocyte recruitment, and up-regulation of MMP-12 and NE expression. Exogenous SIgA replacement reduces lung inflammation in response to bacterial lysates, thus showing a direct anti-inflammatory effect of SIgA in the lungs. Chronic lung inflammation in $pIgR^{-/-}$ mice is abrogated by germ-free housing, implicating bacterial invasion into SIgA-deficient airways as the central driver of inflammation in $pIgR^{-/-}$ mice. Long-term treatment with the anti-inflammatory drug roflumilast blocks progressive small airway wall remodeling and partially reverses emphysematous changes in SIgA-deficient mice with established disease, showing that inflammatory cells and mediators are responsible for COPD-like remodeling. In addition, we found that long-term CS treatment of WT mice resulted in a COPD-like phenotype that was similar in magnitude to the spontaneous phenotype in age-matched $pIgR^{-/-}$ mice. Together with prior publications showing widespread airway surface SIgA deficiency in COPD patients (61, 85) our data support the concept that reduced pIgR expression and acquired SIgA deficiency in the airways of humans contribute to chronic inflammation and disease progression in COPD.

It has long been appreciated that remodeling of small resistance airways is an important determinant of airflow obstruction (25, 27). Our data help to explain the central role of small

airways in COPD. We propose that leukocytes recruited to small airways with acquired SIgA deficiency produce proteases that damage the airway walls, resulting in fibrotic remodeling and ultimately airflow obstruction. In addition, products of activated leukocytes, including MMP-12, and NE, can cause destruction of elastin fibers and other components of the interalveolar septum adjacent to these small airways, leading to centrilobular emphysema. While reduced pIgR expression and SIgA levels in COPD patient airways correlates with abnormal epithelial differentiation (61), the mechanism responsible for reduced pIgR expression and acquired SIgA deficiency in COPD is uncertain and is an important area for further study. Once individual small airways develop pIgR/SIgA deficiency, our data suggest that inflammation may become self-perpetuating, potentially explaining the persistence of airway inflammation in COPD patients after smoking cessation (48, 49).

Our studies indicate that the lung microbiota drives chronic lung inflammation and remodeling in the setting of defective mucosal immunity. While pIgR$^{-/-}$ mice did not show evidence for widespread bacterial overgrowth in the lungs, these mice have increased bacterial invasion across the apical epithelial surface of small airways. In initial studies, we noted an expansion in Alphaproteobacteria and higher community diversity in pIgR$^{-/-}$ mice. Our analysis suggests that a number of OTUs may discriminate between WT and pIgR$^{-/-}$ mice; however, expansion of these findings using a much larger cohort will be required for more definitive conclusions. These data do not exclude the possibility that systemic effects of an altered gut microbiome in pIgR$^{-/-}$ mice could also contribute to the development of lung remodeling. Future studies should determine the composition of the murine lung and gut microbiome prior to and after the development of lung remodeling in WT and pIgR$^{-/-}$ mice and investigate whether the microbiome of pIgR$^{-/-}$ mice is intrinsically more inflammatory than that of WT mice.

In addition to bacteria, viruses and environmental antigens could also impact chronic inflammation and COPD-like remodeling in the setting or mucosal immune deficiency. In intestinal epithelial cells, pIgR is upregulated by dsRNA via TLR3, consistent with a role in

protection against viruses (148). We have previously shown that SIgA-deficient airways have increased expression of CMV late antigen and EBV latent membrane protein compared to SIgA-replete airways from the same individual (61). While colonizing bacteria appear to be the most important driver of COPD-like lung remodeling in pIgR$^{-/-}$ mice housed in the protected environment of our animal care facility, environmental antigens and viruses could also be important drivers of inflammation and progressive disease in COPD patients with acquired SIgA deficiency in small airways.

We found that roflumilast blocks inflammatory cell recruitment and prevents small airway wall remodeling and emphysema that develop in response to pIgR/SIgA deficiency. Roflumilast reduces inflammation in the lungs of COPD patients and is FDA-approved for use in patients with severe COPD (149), where it has been shown to reduce disease exacerbations. Our studies, however, suggest that roflumilast could have a disease-modifying effect in COPD and may be beneficial in patients with less advanced disease.

In our models, pIgR deficiency and long-term CS exposure showed a similar degree of inflammation and COPD-like remodeling in the lungs; however, the combination of pIgR deficiency and cigarette smoking appeared to have an additive effect on small airway wall remodeling and emphysema. This latter finding suggests that the effects of CS and pIgR deficiency are independent in this model. We postulate that the lack of interaction between CS and pIgR/SIgA deficiency may be explained by a lack of structural remodeling of the airway epithelium (e.g. goblet cell hyperplasia or stratification) in our CS model, which may be necessary for repressing pIgR expression. Ganesan and colleagues showed that the combination of chronic CS exposure and bacterial challenge can induce goblet cell hyperplasia, as well as tertiary lymphoid follicles, in mice (150). Studies using combined stimuli that cause structural remodeling of airway epithelium in mice may be necessary to study the effects of acquired pIgR/SIgA deficiency in mouse models.

An implication of our findings is that patients with genetic IgA deficiency, the most common immunodeficiency in humans (151), might be at increased risk for the development of COPD. To our knowledge, no large epidemiologic studies have evaluated whether IgA deficiency is associated with an increased risk for COPD. However, patients with genetic IgA deficiency have normal or even increased levels of IgM (152, 153), which may compensate for lack of SIgA in small airways. In contrast, reduced pIgR expression, which is present in airways of COPD patients (61), limits transport of both dimeric IgA and IgM to the airway surface. Nonetheless, future studies to investigate the incidence and progression of obstructive lung disease in IgA deficient individuals could be informative.

In summary, our studies demonstrate that surface SIgA deficiency in small airways of $pIgR^{-/-}$ mice leads to persistent activation of innate immune responses to resident lung microbiota and generation of a phenotype that resembles important aspects of human COPD. Our findings highlight a critical role for pIgR/SIgA in maintenance of the immune-barrier function of the airway epithelium, and could explain several key aspects of COPD pathogenesis, including the central role of small airways and persistent airway inflammation even after smoking cessation. Therapeutic strategies that restore normal immune barrier function to the small airways or deplete the airways of bacteria may be of therapeutic benefit to patients with COPD.

V. ROFLUMILAST ABROGATES NON-TYPEABLE HAEMOPHILUS INFLUENZA-INDUCED INFLAMMATION AND REMODELING IN PIGR$^{-/-}$ MICE

Results

INCREASED INFLAMMATION AND REMODELING IN PIGR$^{-/-}$ MICE TREATED WITH REPETITIVE BACTERIAL LYSATES

We first established the dose of NTHi lysate required to generate a robust inflammatory response in WT mice. We found that a dose of 10 mg of NTHi lysate, administered via nebulization, resulted in a marked increase in bronchoalveolar lavage (BAL) fluid neutrophils and macrophages at 24 hours in WT mice (**Figure 16A-B**). Further, we used an established (120, 122) non-invasive *in vivo* molecular imaging technique to show that macrophages recruited the the lungs of NTHi-exposed mice had increased expression of folate receptor-β (FR-β), a marker of activation (**Figure 16C-D**). We then treated 2 month-old adult WT or pIgR$^{-/-}$ mice (both C57Bl/6 background) with 10 mg of aerosolized NTHi lysates once weekly for 4 months and measured neutrophil, macrophage, and lymphocyte numbers in BAL fluid. In agreement with our earlier data (**Figure 6**) (122), saline-treated pIgR$^{-/-}$ mice had significantly higher numbers of BAL neutrophils and macrophages than saline-treated WT mice, confirming that pIgR$^{-/-}$ mice spontaneously develop increased numbers of inflammatory cells in the airways (**Figure 17A-B**). Compared to NTHi-treated WT mice, NTHi-treated pIgR$^{-/-}$ mice had a 1.8, 2.5, and 1.9-fold increase in BAL neutrophils, macrophages, and lymphocytes, respectively ($p<0.05$ for all), implicating loss of the SIgA immunobarrier as a potentiator of chronic inflammation in mice serially exposed to bacterial products (**Figure 17A-C**).

In patients with COPD and animal models, proteases produced by inflammatory cells have been linked to fibrotic remodeling of small airways and emphysematous lung destruction (27, 44, 45, 61, 122). Thus, we reasoned that increased numbers of inflammatory cells in NTHi-treated pIgR$^{-/-}$ mice would be associated with more severe lung damage. Using established

methods of morphometric analysis (27, 154), we found that NTHi-exposed pIgR$^{-/-}$ mice had significantly more severe small airway wall thickening and emphysema than NTHi-exposed WT mice, suggesting that higher numbers of inflammatory cells in these mice resulted in greater damage to the airways and lung parenchyma (**Figure 18A-D**). Together, these data show that loss of the SIgA immunobarrier results in increased inflammation and lung remodeling *in vivo* in response to repetitive challenge with bacterial products.

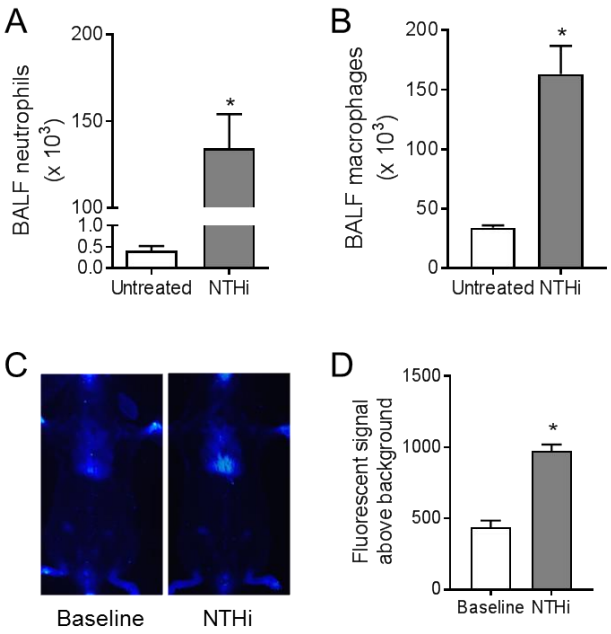

Figure 16: Acute inflammatory response to NTHi lysates in WT mice.

A, B) BALF neutrophil and macrophage counts in WT mice 24 hours after nebulization with NTHi lysates. 6-8 mice/group; * = p<0.001. **C**) Representative images of folate-PEG-Cy5-derived chest fluorescence in WT mice 24 hours after nebulization with NTHi lysates. **D**) Photon emission from the chest 4 hours after probe injection normalized to background prior to probe injection. Three-7 mice/group; * = p<0.001 (Student's *t*-test).

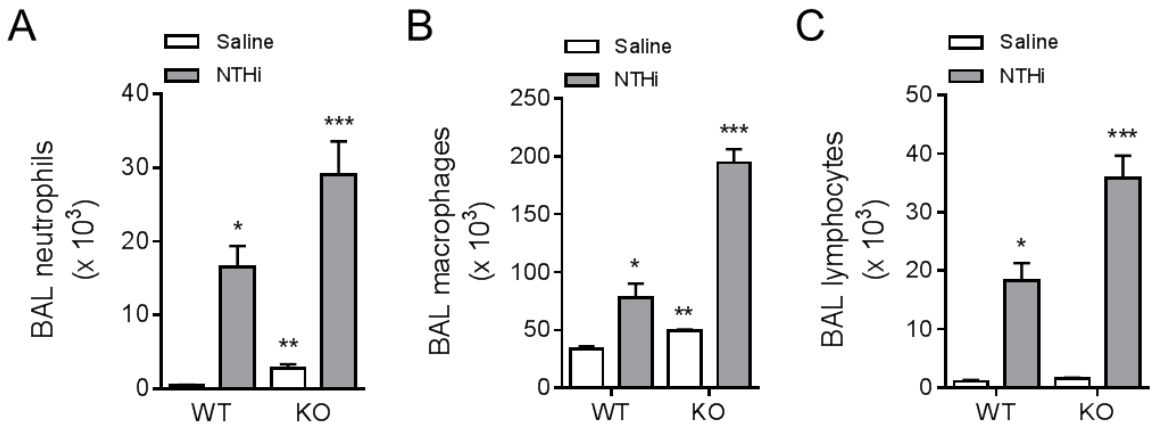

Figure 17: Increased lung inflammation in pIgR$^{-/-}$ mice serially exposed to nebulized NTHi lyates.

A) Neutrophil, **B**) macrophage, and **C**) lymphocyte counts in BAL fluid from WT and pIgR$^{-/-}$ mice treated with nebulized sterile saline or NTHi once weekly for 4 months. Five-7 mice/group. * = $p<0.01$ compared to saline-treated WT mice; ** = $p<0.01$ compared to saline-treated WT mice; *** = $p<0.05$ compared to NTHi-treated WT mice and $p<0.001$ compared to saline-treated pIgR$^{-/-}$ mice (Student's *t*-test).

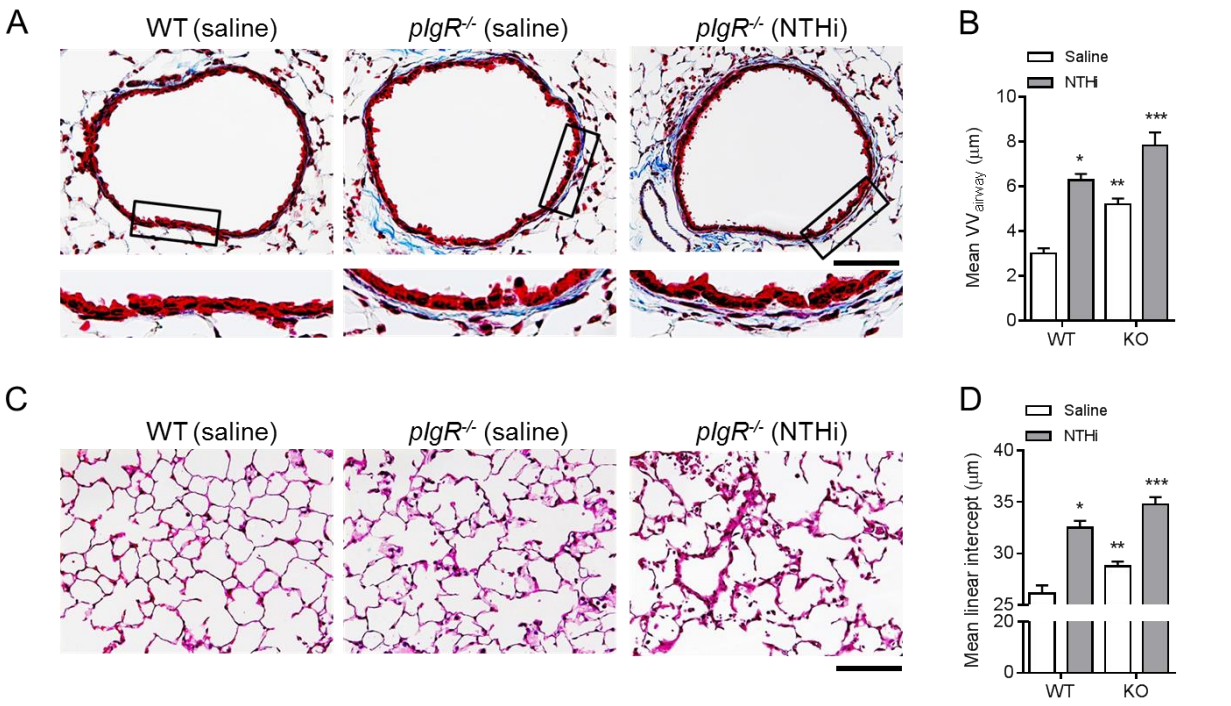

Figure 18: Increased lung remodeling in pIgR$^{-/-}$ mice serially exposed to NTHi lysates.

A) Representative image of small airway wall fibrosis (Masson's trichrome stain) in a WT or pIgR$^{-/-}$ mouse treated with nebulized saline only and a pIgR$^{-/-}$ mouse treated with repetitive NTHi lysates (top row, original magnification x 200; bottom row original magnification x 1000). Subepithelial collagen deposition is indicated by blue staining. Scale bar = 50 μM. **B**) Morphometric analysis showing increased wall thickness (VV_{airway}) in pIgR$^{-/-}$ mice treated with NTHi lysates compared to saline-treated pIgR$^{-/-}$ mice or WT mice treated with NTHi lysates. Five-12 mice/group. * = p<0.0001 compared to saline-treated WT mice; ** = p<0.0001 compared to saline-treated WT mice; *** = p<0.05 compared to NTHi-treated WT mice and p<0.001 compared to saline-treated pIgR$^{-/-}$ mice (Student's *t*-test). **C**) Representative image of emphysema (H&E) in a WT or pIgR$^{-/-}$ mouse treated with nebulized saline only and a pIgR$^{-/-}$ mouse treated with repetitive NTHi lysates (original magnification x 200). Scale bar = 50 μM. **D**) Morphometric analysis showing increased wall thickness (mean linear intercept, MLI) in pIgR$^{-/-}$ mice treated with NTHi lysates compared to saline-treated pIgR$^{-/-}$ mice or WT mice treated with NTHi lysates. Eleven-12 mice/group. * = p<0.0001 compared to saline-treated WT mice; ** = p<0.01 compared to saline-treated WT mice; *** = p<0.05 compared to NTHi-treated WT mice and p<0.0001 compared to saline-treated pIgR$^{-/-}$ mice (Student's *t*-test).

ROFLUMILAST PROTECTS AGAINST NTHI-MEDIATED LUNG REMODELING

We previously demonstrated that spontaneous lung inflammation and remodeling in *pIgR*$^{-/-}$ mice could be abrogated by anti-inflammatory treatment with the phosphodiesterase-4 inhibitor roflumilast. Roflumilast is currently FDA-approved for the treatment of severe COPD in patients with recurrent exacerbations, and has been shown to reduce inflammation in patients and murine models of COPD (143-146). Further, we previously established that roflumilast could block inflammation and lung remodeling in pIgR$^{-/-}$ mice (**Figures 13 and 14**) (122). To determine whether roflumilast is capable of blocking inflammation and remodeling induced by repetitive administration of NTHi lysates, we treated 2 month-old WT or *pIgR*$^{-/-}$ mice daily by oral gavage with 100 μg of roflumilast (5 μg/g) or vehicle (5% methylcellulose, 1.3% PEG400) for four months concurrently with weekly NTHi nebulization. Roflumilast treatment resulted in reduced numbers of inflammatory cells in WT and pIgR$^{-/-}$ mice (**Figure 19A-C**). In pIgR$^{-/-}$ mice, roflumilast-treated animals had a 57% reduction in BAL neutrophils, a 47% reduction in BAL macrophages, and 49% reduction in BAL lymphocytes compared to vehicle-treated animals ($p<0.01$ for all). Further, we found that roflumilast treatment resulted in a 42% reduction in small airway wall thickness (VV_{airway}) and an 18% reduction in mean linear intercept in pIgR$^{-/-}$ mice ($p<0.01$ and $p<0.0001$, respectively). These data suggest that roflumilast can effectively block lung inflammation and remodeling in SIgA-deficient mice repetitively exposed to bacterial products.

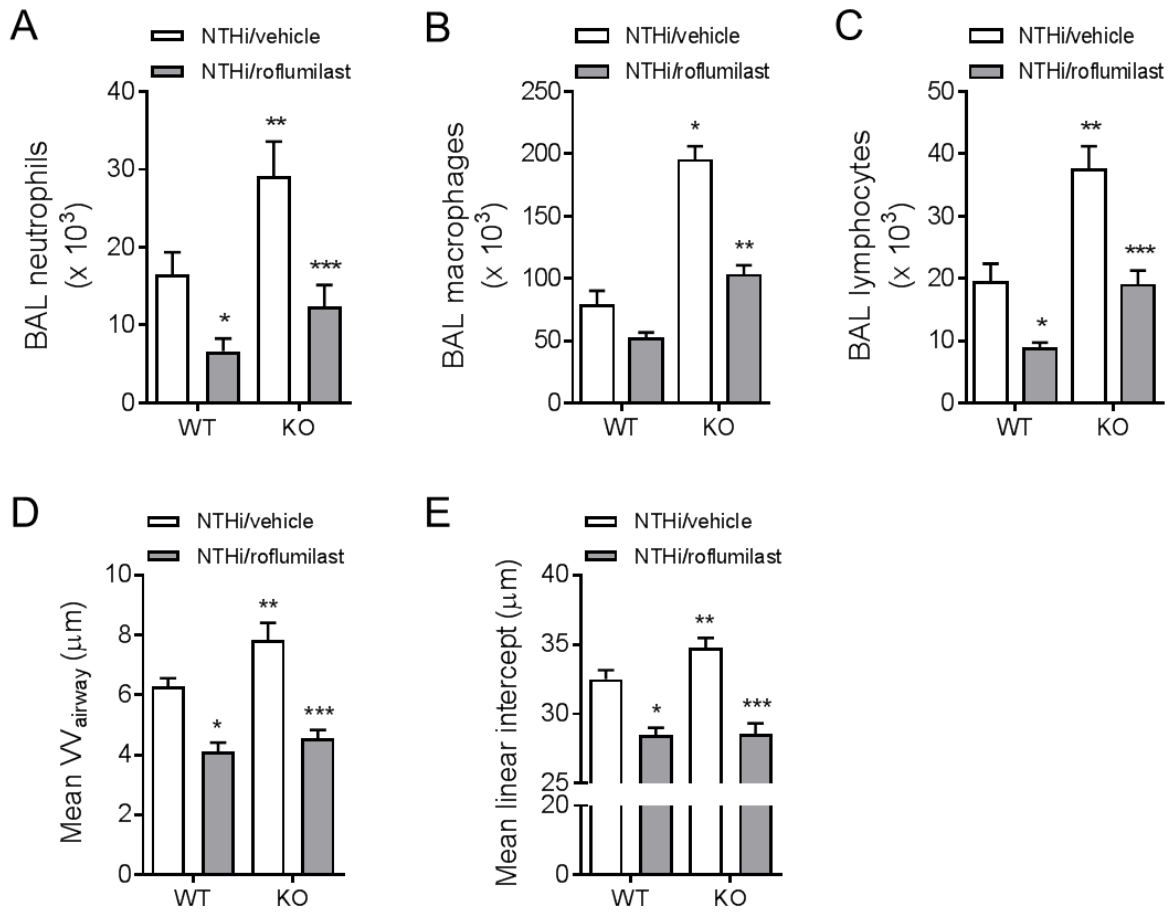

Figure 19: Roflumilast abrogates NTHi-induced inflammation and lung remodeling in mice exposed to NTHi lysates.

A) Neutrophil, **B**) macrophage, and **C**) lymphocyte counts in BAL fluid from WT and pIgR$^{-/-}$ mice treated daily with roflumilast or vehicle for the duration of NTHi exposure (4 months). Six-7 mice/group. * = p<0.05 compared to vehicle-treated WT mice; (B) ** = p<0.05 compared to vehicle-treated WT mice; *** = p<0.01 compared to roflumilast-treated WT mice and p<0.05 compared to vehicle-treated pIgR$^{-/-}$ mice (Student's t-test). **D**) Morphometric analysis of small airway wall thickness (VVairway) in WT and pIgR$^{-/-}$ mice treated daily with roflumilast or vehicle for the duration of NTHi exposure (4 months). Four-5 mice/group. * = p<0.01 compared to vehicle-treated WT mice; ** = p<0.05 compared to vehicle-treated WT mice; *** = p<0.01 compared to vehicle-treated pIgR$^{-/-}$ mice (Student's t-test). (E) Morphometric analysis of emphysema (mean linear intercept) in WT and pIgR$^{-/-}$ mice treated daily with roflumilast or vehicle for the duration of NTHi exposure (4 months). Eleven-12 mice/group. * = p<0.001 compared to vehicle-treated WT mice; ** = p<0.05 compared to vehicle-treated WT mice; *** = p<0.0001 compared to vehicle-treated pIgR$^{-/-}$ mice (Student's t-test).

Discussion

This work establishes that repetitive challenge with bacterial products can potentiate lung inflammation and remodeling in SIgA-deficient mice beyond levels induced by endogenous bacteria, and that anti-inflammatory treatment with roflumilast can effectively reduce lung inflammation and prevent small airway and parenchymal remodeling in a murine model of SIgA-deficiency. These findings suggest that localized SIgA deficiency within small airways may contribute to accelerated lung function decline in patients with COPD who have frequent exacerbations (9) and that roflumilast may have a disease-modifying effect in these patients.

There are several important limitations of this work. First, the use of sterile bacterial lysates rather than live bacteria may underestimate the inflammatory response that would be generated by self-replicating bacteria, and thus overestimate the effectiveness of roflumilast in preventing bacteria-induced airway inflammation and remodeling. Second, we cannot ascertain whether the clinical virulence of a given pathogen influences the magnitude of lung inflammation and remodeling in the setting of SIgA deficiency. In addition, we cannot speculate which bacterial components are most important for driving inflammation in SIgA-deficient airways. Such questions will require testing of a panel of bacteria and/or different bacterial components, ideally in ex vivo models that recapitulate host-pathogen interactions in patients with COPD. Third, because we initiated treatment with roflumilast prior to the development of small airway wall thickening and emphysema, we cannot conclude that roflumilast can prevent further damage induced by bacterial products *in vivo* after lung damage. However, our earlier data (**Figures 13 and 14**) showed that roflumilast can block further disease progression in pIgR$^{-/-}$ mice with established disease resulting from endogenous bacteria.

In summary, these data provide evidence that loss of SIgA in small airways may contribute to the accelerated decline in lung function noted in patients with COPD who have frequent bacterial respiratory infections, and suggest that roflumilast may provide a disease-modifying effect for such patients.

VI. REGULATION OF *PIGR* BY P73

Rationale

As discussed in Chapter II, available evidence suggests that loss of SIgA in the airways of patients with COPD is caused by a transcriptional block in *PIGR* expression associated with abnormal epithelial differentiation (61). Given that airway remodeling in COPD is associated with a loss of airway multiciliated cells (MCCs), we speculated that these cells are unique in their ability to express *PIGR*. A breakthrough in our understanding of the factors regulating *PIGR* expression was recently provided Marshall and colleagues, who used RNA sequencing to show that murine tracheal epithelial cells isolated from mice lacking p73 had reduced *PIGR* expression (117). Functionally null p73 mice had almost a complete absence of MCCs, suggesting that p73 is a central regulator of MCC differentiation and providing additional evidence that MCCs are unique in their ability to express pIgR. Marshall and colleagues went on to show that p73 binds a variety of transcription factors required for MCC differentiation including Myb, FoxJ1, and Traf3ip1 (117). In a similar study, Nemajerova et al. confirmed the findings of Marshall et al. and showed that p73 is required for the early events of cilia formation including basal body docking and axonemal extension (118). Given the importance of p73 in MCC differentiation, we speculated that loss of p73 might explain the reduction in ciliated cells and *PIGR* expression we previously noted in the small airways of patients with COPD (61).

Results

LOSS OF MCCS IS ASSOCIATED WITH REDUCED SIGA AND P73 IN THE AIRWAYS OF COPD PATIENTS

To determine the relationship between p73, numbers of MCCs, and SIgA transcytosis in human airways, we performed immunostaining for α-tubulin and p73 (marking MCCs) and SIgA using lung sections from patients with COPD. As shown in **Figure 20A**, airways covered

predominantly by α-tubulin/p73-expressing MCCs maintained an intact SIgA immunobarrier, while airways with few or no MCCs had virtually no SIgA.

Further, there was a significant correlation between the percentage of airway epithelium occupied by ciliated cells and the intensity of IgA staining (as measured by actual pixel value, apv); and the percentage of airway epithelium occupied by p73+ cells (**Figure 20B-C**). These data suggest that MCCs are critical for maintenance of the SIgA immunobarrier, and extend *in vivo* studies by Marshall et al. and Nemajerova et al. to show that in human airways loss of MCCs and p73 expression are interrelated.

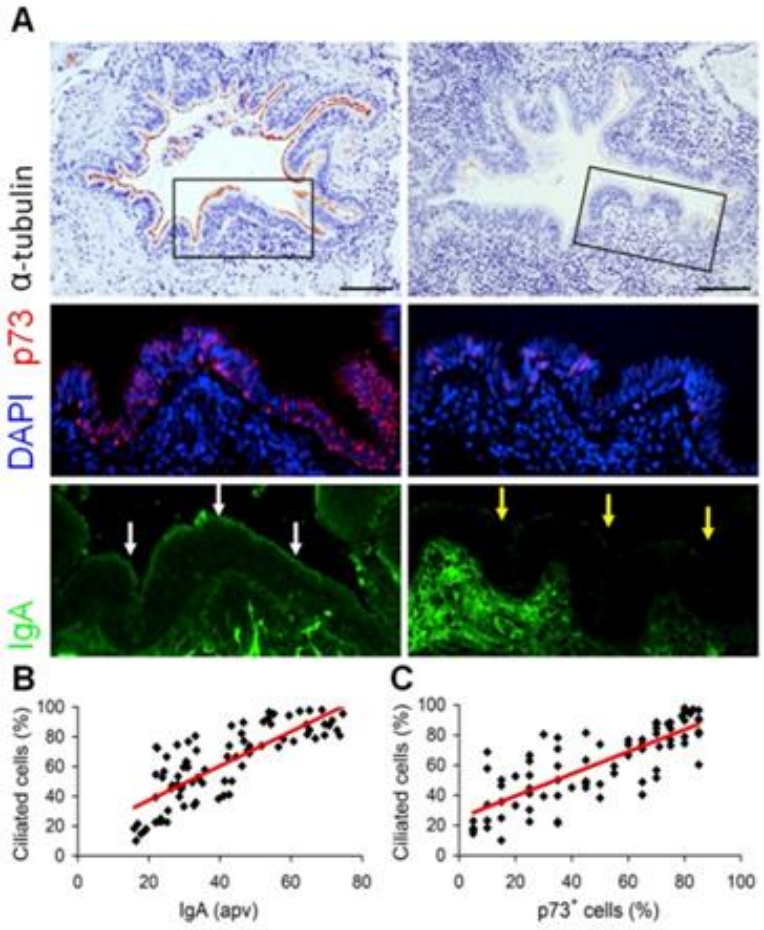

Figure 20: p73-expressing MCCs are reduced in SIgA-deficient airways from COPD patients.

A) Immunostaining for α-tubulin to detect MCCs, p73, and IgA in airways from a COPD patient. White and yellow arrows show the edge of the epithelium in a SIgA replete and SIgA-deficient airway, respectively. Arrows indicate the mucosal surface. Scale bar = 100 μM. **B**) Correlation between percentage of ciliated cells by α-tubulin staining and IgA level (absolute pixel value, apv) on the surface of 83 individual airways of 5 patients with COPD. r = 0.79, $p<0.01$. **C**) Correlation between percentage of ciliated cells and percentage of p73+ cells in individual airways. r = 0.74, $p<0.01$.

p73$^{-/-}$ MICE LACK pIgR IN SMALL AIRWAYS

We next obtained p73$^{fl/fl}$ mice (C57Bl6/J background) which contain loxP sites flanking exons 7-9 of *TP73*. These mice were crossed with mice in which Cre is ubiquitously expressed (CMV.Cre), such that the resulting progeny lacked the DNA-binding domain, nuclear localization signal, and oligomerization domain of *TP73*. In accordance with the findings of Marshall et al., murine tracheal epithelial cells from these functionally null (p73$^{-/-}$) mice had almost a complete absence of pIgR, as determined by immunostaining (**Figure 21A**). Further, we found that pIgR is co-expressed with FoxJ1 (a marker for MCCs) in MTECs from WT mice (**Figure 21B**), supporting the idea that MCCs are the source of pIgR expression in murine airways.

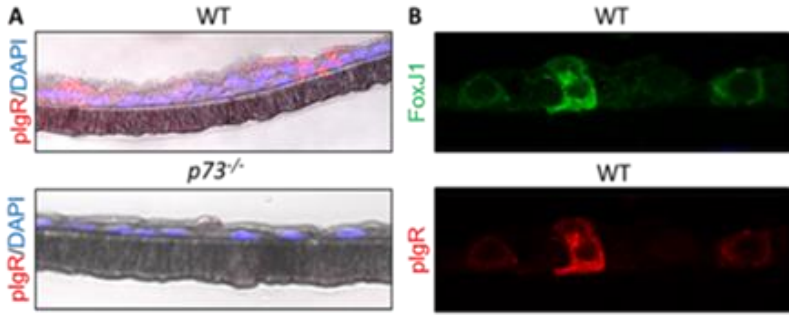

Figure 21: p73 is a critical regulator of pIgR expression in mouse airway epithelial cells.

A) Immunostaining for pIgR in MTECs isolated from WT or $p73^{-/-}$ mice. $p73^{-/-}$ cells are characterized by lack of cilia and no detectable pIgR staining (400X). **B**) Co-immunofluorescence shows that pIgR expressing cells are also FoxJ1 positive.

DEFICIENCY OF PIGR OR P73 LEADS TO PROGRESSIVE COPD-LIKE PATHOLOGY IN MICE

In Chapter IV, we showed that pIgR$^{-/-}$ mice, which lack SIgA in the airways, spontaneously develop small airway and lung parenchymal inflammation and remodeling by 6 months of age (122). Further studies showed that loss of the protective SIgA immunobarrier in pIgR$^{-/-}$ mice is associated with increased bacterial invasion into small airways, and that re-derivation of pIgR$^{-/-}$ mice into germ-free housing prevents these mice from developing lung inflammation and remodeling (122). More recently, we found that a 4-drug antibiotics cocktail administered in drinking water (vancomycin, neomycin, ampicillin, and metronidazole, "VNAM") could halt the development of COPD-like small airway remodeling and emphysema in pIgR$^{-/-}$ mice (data not shown). These studies suggest that the COPD-like phenotype observed in pIgR$^{-/-}$ mice is caused by bacterial penetration into SIgA-deficient airways.

After noting that loss of MCCs is associated with reduced airway SIgA in patients with COPD (**Figure 21A**), we speculated that p73 deficient mice (which lack MCCs) would display reduced airway SIgA and would spontaneously develop bacterial invasion and COPD-like lung remodeling similar to pIgR$^{-/-}$ mice. Airways from 12 month-old p73$^{-/-}$ mice had almost no detectable pIgR expression and lacked IgA on the airway surface (**Figure 22A**). Bacterial DNA was frequently detectable within the epithelial layer of airways from p73$^{-/-}$ mice (15.4% of airways in cross section) and NF-κB activation was apparent in the airway epithelium of almost all airways (**Figure 22A**).

Similar to age-matched pIgR$^{-/-}$ mice, 12 month-old p73$^{-/-}$ mice were noted to have extensive airway fibrotic remodeling (as measured by subepithelial connective tissue volume density, VV_{airway}) and emphysema (as measured by mean linear intercept, MLI) (**Figure 22B-C**). However, the pathology in p73$^{-/-}$ is even more severe than in pIgR$^{-/-}$ mice, suggesting that other abnormalities related to loss of MCCs likely contribute to the COPD phenotype in these mice. Together, our data support the model that loss of p73 prevents the development of MCCs, which are critical for pIgR expression, SIgA delivery, and mucosal homeostasis in the airways.

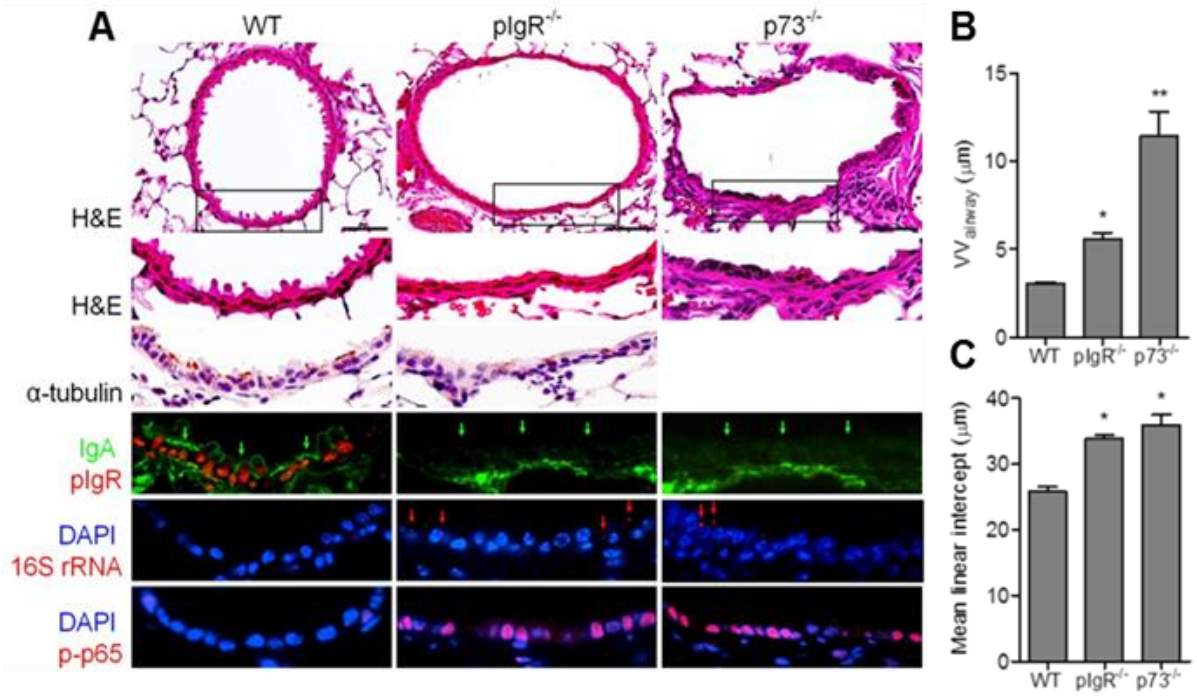

Figure 22: pIgR$^{-/-}$ and p73$^{-/-}$ mice have absent pIgR/SIgA and increased bacterial invasion and NF-κB activation in the airways.

A) Serial sections from lungs of 12 month-old WT, pIgR$^{-/-}$, and p73$^{-/-}$ mice were stained with H&E or immunostained with antibodies to α-tubulin, IgA, pIgR, NF-κB [phospho-p65 (Ser276)], or bacterial 16S rRNA (by FISH). Both pIgR$^{-/-}$, and p73$^{-/-}$ mice have reduced MCCs and SIgA on the airway surface that is associated with bacterial invasion into the epithelial barrier and NF-κB activation. Green arrows indicate the mucosal surface; red arrows indicate bacteria invading into the mucosa. Scale bar = 50 μM. **B, C**) Morphometric analysis of small airway fibrotic remodeling (VV_{airway}) and emphysema (mean linear intercept) in12 month-old WT, pIgR$^{-/-}$, and p73$^{-/-}$ mice.

CIGARETTE SMOKE SUPPRESSES P73 *IN VITRO* AND *IN VIVO*

Given the association between cigarette smoking and COPD, we questioned whether cigarette smoke exposure affects p73 expression. Therefore, we grew MTECs to confluence in submerged culture, transferred to air-liquid interface (ALI) culture to promote differentiation, and then added fresh cigarette smoke extract (CSE, 2.5% v/v in culture media) or vehicle (phosphate-buffered saline, PBS) daily from Day 2 to Day 16 in ALI culture. CSE was generated by bubbling a combination of mainstream and sidestream smoke produced by three 3R4F Research Cigarettes (Reference Cigarette Program, University of Kentucky, Lexington, KY) though PBS. After 16 days in ALI culture, we fixed the cells and performed immunostaining for pIgR and p73. As shown in **Figure 23A**, MTECs treated with CSE had a marked reduction in pIgR and p73 staining. To test the relationship between CS exposure and p73 expression in the airways, we exposed WT mice to mainstream CS for 2 weeks. For this study, mice were placed in a nose-only smoke exposure chamber (inExpose system, EMKA/SCIREQ, Tempe, AZ) and treated with two cigarettes once daily for 5 days followed by four cigarettes twice daily (5 days/week) for 2 weeks. As shown in **Figure 23B**, untreated mice had diffuse p73 and pIgR staining in the airway epithelium. In contrast, CS-treated mice had reduced expression of both p73 and pIgR, along with activation of NF-κB. The finding of reduced pIgR was confirmed by western blot from whole lung lysates and SIgA levels were reduced in BAL (**Figure 23C-D**).

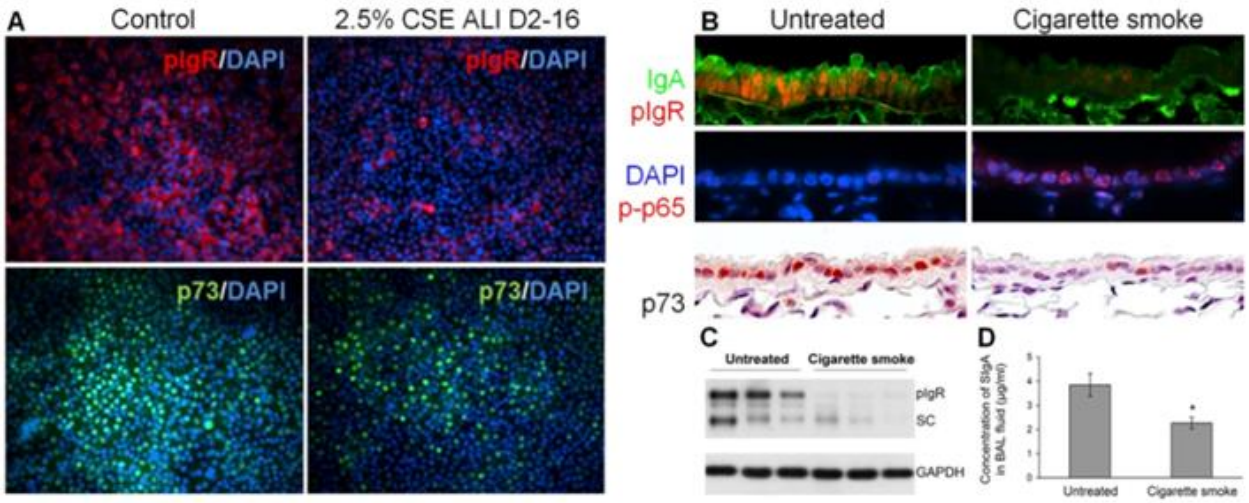

Figure 23: Cigarette smoke suppresses pIgR and p73 *in vitro* and *in vivo*.

A) Immunostaining for pIgR or p73 and DAPI in WT MTECS treated daily from Day 2 to Day 16 in ALI culture with 2.5% CSE or vehicle (control) (20X). **B-D**) Studies from untreated WT mice and WT mice exposed to cigarette smoke daily for 2 weeks (as described in text). **B**) Immunofluorescent detection of IgA (green) and pIgR (red) (top panels), NF-κB [phospho-p65 (Ser276)] (red) and DAPI (blue) (middle panels), and immunostaining for p73 (brown, bottom panels) in WT mice treated with CS or controls. **C**) Western blot for pIgR in whole lung lysates. Separate bands for pIgR and secretory component (SC) are identified. GAPDH is shown as a loading control. **D**) SIgA concentration measured by ELISA in BAL fluid. Mean ± SEM, 3 mice per group, *=p<0.05.

INVERSE RELATIONSHIP BETWEEN NF-κB ACTIVATION AND P73 EXPRESSION

Using a transgenic mouse model to express a constitutively active form of IKKβ (enzyme that activates classical NF-κB signaling) in airway epithelium, our group recently showed that chronic activation of NF-κB results in a severe COPD-like phenotype with airway wall remodeling, and diffuse emphysema (155). Since NF-κB has been reported to decrease p73 by targeting it for proteasomal destruction (156, 157), we wondered whether NF-κB-driven signaling suppresses p73 *in vivo*. Therefore, we evaluated p73 expression in these IKKβ-transactivated mice (IKTA) mice (155, 158). We found that 4 month-old IKTA mice treated for 2 months with doxycycline had nearly a total absence MCCs (indicated by absent α-tubulin staining) as well as p73 and pIgR staining in small airways (**Figure 24A**). To test whether NF-κB can downregulate p73 in epithelial cells, we cultured MDA-MB-231 adenocarcinoma cells which express p73 under basal conditions (159). We treated these cells with TNFα to activate NF-κB signaling and observed a substantial reduction in p73 at 24 hours (**Figure 24B**), suggesting an inverse relationship between NF-κB pathway activation and p73 expression *in vitro*.

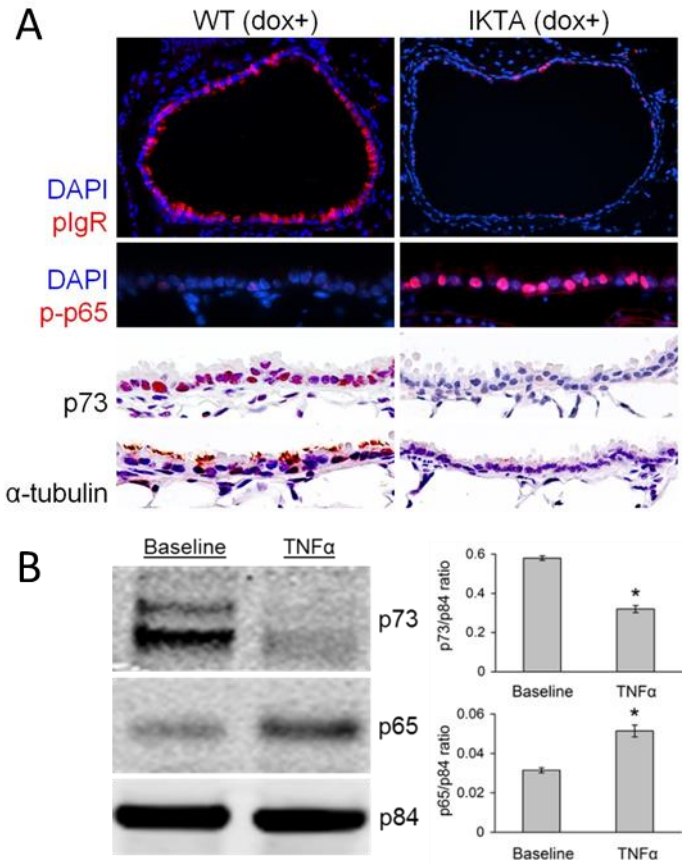

Figure 24: Inverse relationship between p73 and NF-κB activation

A) Immunostaining for pIgR, phospho-NF-κB (Ser276), p73, α-tubulin, and pIgR in lung sections from 4 month-old IKTA mice with and without dox treatment. There is virtually a complete lack of p73, α-tubulin, and pIgR staining in the small airways of IKTA mice with the IKTA transgene activated (200X, insets 1000X). **B**) MDA-MB-231 cells were treated with TNFα (40 ng/ml) for 24 h. Western blots were done from nuclear protein extracts for NF-κB p65 (Ser276), p73, and p84 (loading control). n=4 separate experiments, *=p<0.01.

Discussion

Abnormal differentiation of the airway epithelium, including loss of ciliated cells and hyperplasia of basal and goblet cells, is a hallmark of COPD (54). Here we show that the differentiation factor p73, recently found to be required for multiciliated cell differentiation (117, 118), is required for pIgR expression. This suggests that multiciliated cells are unique in their ability to express pIgR and maintain the SIgA immunobarrier. We found that cigarette smoke exposure reduces p73 expression *in vitro* and *in vivo*. These data suggest that p73 may be a crucial factor in the process through which chronic cigarette smoke exposure induces abnormal epithelial differentiation. Further, we found an inverse relationship between NF-κB pathway activation and p73 expression, suggesting that chronic inflammation resulting from loss of SIgA in the airways may perpetuate abnormal epithelial differentiation once it is established by cigarette smoke exposure. Finally, we found that p73 is reduced in the airways of patients with COPD, reflecting the loss of ciliated cells in these airways and potentially explaining the persistence of abnormal airway remodeling in COPD.

VII. Concluding Remarks and Future Directions

In summary, this work provides a new conceptual framework for understanding how inflammation persists in the small airways of patients with COPD, driving ongoing lung damage after smoking cessation. In the setting of epithelial remodeling, which is pervasive in COPD , the airway epithelium is no longer able to generate a normal SIgA immunobarrier, resulting in bacterial penetration into the airways, triggering of inflammatory signaling pathways in epithelial cells, neutrophil and macrophage recruitment, protease/antiprotease imbalance, and ultimately small airway remodeling and emphysema. Thus we have defined localized SIgA deficiency in small airways as a driver of protease/antiprotease imbalance and disease progression in COPD. In addition, our work suggests that multiciliated cells (MCCs) are unique in their ability to express pIgR, and that the MCC differentiation factor p73 is required for pIgR expression. Our work suggests that p73 levels are modulated by cigarette smoke *in vitro* and *in vivo*, which may explain how cigarette smoke initiates abnormal epithelial differentiation in COPD. Finally, our work suggests that inflammation per se may suppress p73, which may explain why abnormal epithelial differentiation persists in SIgA-deficient airways after smoking cessation.

While the current work focused on the role of airway bacteria in driving inflammation *in vivo*, it is important to recognize that SIgA is also important for the immune response to viruses and non-infectious irritants, and thus infection or reactivation of viruses or chronic exposure to inhaled irritants may also drive inflammation in SIgA-deficient airways. This is an important question that must be answered prior to considering strategies to deplete or modulate airway bacteria as a therapeutic strategy. Further, our studies into the impact of SIgA on the composition of the microbiome should be considered preliminary. Future studies will be needed to confirm our observed effects of SIgA deficiency on the lung microbiome in a larger cohort, ideally with comparisons between the effects of tissue-specific deletion of SIgA in the lung and gut on the lung microbiome.

In this dissertation, we focused on how the innate immune system contributes to COPD pathogenesis in the setting of SIgA deficiency. However, patients with COPD also have activation of the adaptive immune system, as evidenced by an accumulation of CD8+ T lymphocytes, CD4+ (predominantly Th1) T lymphocytes, and B lymphocytes (27, 160-163). Lymphocytic infiltration of the lung persists long after smoking cessation and is thought to contribute to the development of emphysema by stimulating alveolar cell apoptosis (50). We speculate that chronic activation of the adaptive immune system may result from increased bacterial penetration into SIgA-deficient airways. In support of this idea, B cells from lymphoid follicles are oligoclonal, suggesting an antigen-driven selection process (164). Future studies will be required to determine whether adaptive immune cells accumulate preferentially in SIgA-deficient airways and contribute to airway and parenchymal damage.

Loss of multiciliated cells is a hallmark of abnormal epithelial differentiation in COPD. While the finding that $p73^{-/-}$ mice have nearly absent MCCs and pIgR provides indirect evidence that MCCs are unique in their ability to express pIgR, this has not been tested directly. Future experiments using co-localization microscopy and cell-type specific deletion of *PIGR* will be required to confirm that only ciliated cells are capable of producing pIgR under homeostatic conditions and in response to injury. Further, additional studies will be required to determine whether p73 regulates *PIGR* directly, through a transcriptional intermediate such as FoxJ1, or indirectly through preferential selection of ciliated versus secretory lineages.

Finally, our work shows that cigarette smoke suppresses p73 production *in vitro* and *in vivo*. This is an intriguing finding that might explain how cigarette smoke initiates abnormal epithelial remodeling in COPD. Future studies will be required to determine whether cigarette smoke suppresses p73 at the mRNA or protein level, establish the minimum dose and duration of exposure that is required to suppress p73 *in vivo*, elucidate whether p73 re-appears following smoking cessation, and identify the mechanism(s) through which cigarette smoke-mediated p73 suppression occurs. Prior work has suggested that NF-κB reduces p73 by targeting it for

proteasomal destruction (156, 157). Consistent with this work, we found that mice with constitutive activation of NF-κB in the airway epithelium have reduced p73. If p73 suppression is inversely related to airway inflammation *per se*, this finding could suggest that p73 serves as a checkpoint to prevent MCC differentiation in severely injured airways, perhaps in order to fully repopulate the airway epithelium with multipotent progenitor cells.

In summary, this work identifies altered mucosal immunity as a driver of chronic inflammation and disease progression in COPD. This will hopefully lead to the development of new therapies for this common and incurable disease.

REFERENCES

1. Kochanek KD, Xu J, Murphy SL, Minino AM, Kung HC. Deaths: final data for 2009. National vital statistics reports : from the Centers for Disease Control and Prevention, National Center for Health Statistics, National Vital Statistics System. 2011;60(3):1-116. PubMed PMID: 24974587.

2. Lozano R, Naghavi M, Foreman K, Lim S, Shibuya K, Aboyans V, et al. Global and regional mortality from 235 causes of death for 20 age groups in 1990 and 2010: a systematic analysis for the Global Burden of Disease Study 2010. Lancet. 2012;380(9859):2095-128. doi: 10.1016/S0140-6736(12)61728-0. PubMed PMID: 23245604.

3. Ford ES, Murphy LB, Khavjou O, Giles WH, Holt JB, Croft JB. Total and state-specific medical and absenteeism costs of COPD among adults aged >/= 18 years in the United States for 2010 and projections through 2020. Chest. 2015;147(1):31-45. doi: 10.1378/chest.14-0972. PubMed PMID: 25058738.

4. From the Global Strategy for the Diagnosis, Management and Prevention of COPD, Global Initiative for Chronic Obstructive Lung Disease (GOLD) 2016. Available from: http://goldcopd.org/.

5. Soler-Cataluna JJ, Martinez-Garcia MA, Roman Sanchez P, Salcedo E, Navarro M, Ochando R. Severe acute exacerbations and mortality in patients with chronic obstructive pulmonary disease. Thorax. 2005;60(11):925-31. doi: 10.1136/thx.2005.040527. PubMed PMID: 16055622; PubMed Central PMCID: PMC1747235.

6. Calverley PM, Anderson JA, Celli B, Ferguson GT, Jenkins C, Jones PW, et al. Salmeterol and fluticasone propionate and survival in chronic obstructive pulmonary disease.

The New England journal of medicine. 2007;356(8):775-89. doi: 10.1056/NEJMoa063070. PubMed PMID: 17314337.

7. Seemungal TA, Donaldson GC, Paul EA, Bestall JC, Jeffries DJ, Wedzicha JA. Effect of exacerbation on quality of life in patients with chronic obstructive pulmonary disease. American journal of respiratory and critical care medicine. 1998;157(5 Pt 1):1418-22. doi: 10.1164/ajrccm.157.5.9709032. PubMed PMID: 9603117.

8. Seemungal TA, Donaldson GC, Bhowmik A, Jeffries DJ, Wedzicha JA. Time course and recovery of exacerbations in patients with chronic obstructive pulmonary disease. American journal of respiratory and critical care medicine. 2000;161(5):1608-13. doi: 10.1164/ajrccm.161.5.9908022. PubMed PMID: 10806163.

9. Donaldson GC, Seemungal TA, Bhowmik A, Wedzicha JA. Relationship between exacerbation frequency and lung function decline in chronic obstructive pulmonary disease. Thorax. 2002;57(10):847-52. PubMed PMID: 12324669; PubMed Central PMCID: PMC1746193.

10. Seemungal TA, Hurst JR, Wedzicha JA. Exacerbation rate, health status and mortality in COPD--a review of potential interventions. International journal of chronic obstructive pulmonary disease. 2009;4:203-23. PubMed PMID: 19554195; PubMed Central PMCID: PMC2699821.

11. Ezzati M, Lopez AD. Estimates of global mortality attributable to smoking in 2000. Lancet. 2003;362(9387):847-52. doi: 10.1016/S0140-6736(03)14338-3. PubMed PMID: 13678970.

12. Eisner MD, Anthonisen N, Coultas D, Kuenzli N, Perez-Padilla R, Postma D, et al. An official American Thoracic Society public policy statement: Novel risk factors and the global

burden of chronic obstructive pulmonary disease. American journal of respiratory and critical care medicine. 2010;182(5):693-718. doi: 10.1164/rccm.200811-1757ST. PubMed PMID: 20802169.

13. Varkey AB. Chronic obstructive pulmonary disease in women: exploring gender differences. Current opinion in pulmonary medicine. 2004;10(2):98-103. PubMed PMID: 15021178.

14. Buist AS, Vollmer WM, McBurnie MA. Worldwide burden of COPD in high- and low-income countries. Part I. The burden of obstructive lung disease (BOLD) initiative. The international journal of tuberculosis and lung disease : the official journal of the International Union against Tuberculosis and Lung Disease. 2008;12(7):703-8. PubMed PMID: 18544191.

15. Silverman EK, Chapman HA, Drazen JM, Weiss ST, Rosner B, Campbell EJ, et al. Genetic epidemiology of severe, early-onset chronic obstructive pulmonary disease. Risk to relatives for airflow obstruction and chronic bronchitis. American journal of respiratory and critical care medicine. 1998;157(6 Pt 1):1770-8. doi: 10.1164/ajrccm.157.6.9706014. PubMed PMID: 9620904.

16. Eriksson S. Pulmonary Emphysema and Alpha1-Antitrypsin Deficiency. Acta medica Scandinavica. 1964;175:197-205. PubMed PMID: 14124635.

17. Zhou JJ, Cho MH, Castaldi PJ, Hersh CP, Silverman EK, Laird NM. Heritability of chronic obstructive pulmonary disease and related phenotypes in smokers. American journal of respiratory and critical care medicine. 2013;188(8):941-7. doi: 10.1164/rccm.201302-0263OC. PubMed PMID: 23972146; PubMed Central PMCID: PMC3826281.

18. Pillai SG, Ge D, Zhu G, Kong X, Shianna KV, Need AC, et al. A genome-wide association study in chronic obstructive pulmonary disease (COPD): identification of two major susceptibility loci. PLoS genetics. 2009;5(3):e1000421. doi: 10.1371/journal.pgen.1000421. PubMed PMID: 19300482; PubMed Central PMCID: PMC2650282.

19. Pillai SG, Kong X, Edwards LD, Cho MH, Anderson WH, Coxson HO, et al. Loci identified by genome-wide association studies influence different disease-related phenotypes in chronic obstructive pulmonary disease. American journal of respiratory and critical care medicine. 2010;182(12):1498-505. doi: 10.1164/rccm.201002-0151OC. PubMed PMID: 20656943; PubMed Central PMCID: PMC3029936.

20. Zhou H, Yang J, Li D, Xiao J, Wang B, Wang L, et al. Association of IREB2 and CHRNA3/5 polymorphisms with COPD and COPD-related phenotypes in a Chinese Han population. Journal of human genetics. 2012;57(11):738-46. doi: 10.1038/jhg.2012.104. PubMed PMID: 22914670.

21. Cho MH, Castaldi PJ, Hersh CP, Hobbs BD, Barr RG, Tal-Singer R, et al. A Genome-Wide Association Study of Emphysema and Airway Quantitative Imaging Phenotypes. American journal of respiratory and critical care medicine. 2015;192(5):559-69. doi: 10.1164/rccm.201501-0148OC. PubMed PMID: 26030696; PubMed Central PMCID: PMC4595690.

22. Kim WJ, Lee SD. Candidate genes for COPD: current evidence and research. International journal of chronic obstructive pulmonary disease. 2015;10:2249-55. doi: 10.2147/COPD.S80227. PubMed PMID: 26527870; PubMed Central PMCID: PMC4621177.

23. Boueiz A, Lutz SM, Cho MH, Hersh CP, Bowler RP, Washko GR, et al. Genome-Wide Association Study of the Genetic Determinants of Emphysema Distribution. American journal of

respiratory and critical care medicine. 2016. doi: 10.1164/rccm.201605-0997OC. PubMed PMID: 27669027.

24. Hogg JC, Timens W. The pathology of chronic obstructive pulmonary disease. Annual review of pathology. 2009;4:435-59. doi: 10.1146/annurev.pathol.4.110807.092145. PubMed PMID: 18954287.

25. Hogg JC, Macklem PT, Thurlbeck WM. Site and nature of airway obstruction in chronic obstructive lung disease. The New England journal of medicine. 1968;278(25):1355-60. doi: 10.1056/NEJM196806202782501. PubMed PMID: 5650164.

26. Yanai M, Sekizawa K, Ohrui T, Sasaki H, Takishima T. Site of airway obstruction in pulmonary disease: direct measurement of intrabronchial pressure. Journal of applied physiology. 1992;72(3):1016-23. PubMed PMID: 1568955.

27. Hogg JC, Chu F, Utokaparch S, Woods R, Elliott WM, Buzatu L, et al. The nature of small-airway obstruction in chronic obstructive pulmonary disease. The New England journal of medicine. 2004;350(26):2645-53. doi: 10.1056/NEJMoa032158. PubMed PMID: 15215480.

28. Jeffery PK. Remodeling and inflammation of bronchi in asthma and chronic obstructive pulmonary disease. Proceedings of the American Thoracic Society. 2004;1(3):176-83. doi: 10.1513/pats.200402-009MS. PubMed PMID: 16113432.

29. Burgel PR. The role of small airways in obstructive airway diseases. European respiratory review : an official journal of the European Respiratory Society. 2011;20(119):23-33. doi: 10.1183/09059180.00010410. PubMed PMID: 21357889.

30. Hogg JC, McDonough JE, Suzuki M. Small airway obstruction in COPD: new insights based on micro-CT imaging and MRI imaging. Chest. 2013;143(5):1436-43. doi: 10.1378/chest.12-1766. PubMed PMID: 23648907; PubMed Central PMCID: PMC3653349.

31. McLean KH. The histology of generalized pulmonary emphysema. I. The genesis of the early centrolobular lesion: focal emphysema. Australasian annals of medicine. 1957;6(2):124-40. PubMed PMID: 13445637.

32. Sharafkhaneh A, Hanania NA, Kim V. Pathogenesis of emphysema: from the bench to the bedside. Proceedings of the American Thoracic Society. 2008;5(4):475-7. doi: 10.1513/pats.200708-126ET. PubMed PMID: 18453358; PubMed Central PMCID: PMC2645322.

33. Silvers GW, Petty TL, Stanford RE. Elastic recoil changes in early emphysema. Thorax. 1980;35(7):490-5. PubMed PMID: 7434309; PubMed Central PMCID: PMC471319.

34. Leopold JG, Gough J. The centrilobular form of hypertrophic emphysema and its relation to chronic bronchitis. Thorax. 1957;12(3):219-35. PubMed PMID: 13467881; PubMed Central PMCID: PMC1019212.

35. Thurlbeck WM. Pathology of chronic airflow obstruction. Chest. 1990;97(2 Suppl):6S-10S. PubMed PMID: 2404712.

36. Laurell CB, Eriksson S. The electrophoretic alpha1-globulin pattern of serum in alpha1-antitrypsin deficiency. 1963. Copd. 2013;10 Suppl 1:3-8. doi: 10.3109/15412555.2013.771956. PubMed PMID: 23527532.

37. Lomas DA, Mahadeva R. Alpha1-antitrypsin polymerization and the serpinopathies: pathobiology and prospects for therapy. The Journal of clinical investigation.

2002;110(11):1585-90. doi: 10.1172/JCI16782. PubMed PMID: 12464660; PubMed Central PMCID: PMC151637.

38. Gross P, Pfitzer EA, Tolker E, Babyak MA, Kaschak M. Experimental Emphysema: Its Production with Papain in Normal and Silicotic Rats. Archives of environmental health. 1965;11:50-8. PubMed PMID: 14312390.

39. Lieberman J. Elastase, collagenase, emphysema, and alpha1-antitrypsin deficiency. Chest. 1976;70(1):62-7. PubMed PMID: 179761.

40. Janoff A, White R, Carp H, Harel S, Dearing R, Lee D. Lung injury induced by leukocytic proteases. The American journal of pathology. 1979;97(1):111-36. PubMed PMID: 495691; PubMed Central PMCID: PMC2042389.

41. Janoff A. Elastases and emphysema. Current assessment of the protease-antiprotease hypothesis. The American review of respiratory disease. 1985;132(2):417-33. doi: 10.1164/arrd.1985.132.2.417. PubMed PMID: 3896082.

42. Lesser M, Padilla ML, Cardozo C. Induction of emphysema in hamsters by intratracheal instillation of cathepsin B. The American review of respiratory disease. 1992;145(3):661-8. doi: 10.1164/ajrccm/145.3.661. PubMed PMID: 1546848.

43. Wright JL, Cosio M, Churg A. Animal models of chronic obstructive pulmonary disease. American journal of physiology Lung cellular and molecular physiology. 2008;295(1):L1-15. doi: 10.1152/ajplung.90200.2008. PubMed PMID: 18456796; PubMed Central PMCID: PMC2494776.

44. Hautamaki RD, Kobayashi DK, Senior RM, Shapiro SD. Requirement for macrophage elastase for cigarette smoke-induced emphysema in mice. Science. 1997;277(5334):2002-4. PubMed PMID: 9302297.

45. Shapiro SD, Goldstein NM, Houghton AM, Kobayashi DK, Kelley D, Belaaouaj A. Neutrophil elastase contributes to cigarette smoke-induced emphysema in mice. The American journal of pathology. 2003;163(6):2329-35. doi: 10.1016/S0002-9440(10)63589-4. PubMed PMID: 14633606; PubMed Central PMCID: PMC1892384.

46. Turino GM. The origins of a concept: the protease-antiprotease imbalance hypothesis. Chest. 2002;122(3):1058-60. PubMed PMID: 12226052.

47. Abboud RT, Vimalanathan S. Pathogenesis of COPD. Part I. The role of protease-antiprotease imbalance in emphysema. The international journal of tuberculosis and lung disease : the official journal of the International Union against Tuberculosis and Lung Disease. 2008;12(4):361-7. PubMed PMID: 18371259.

48. Wright JL, Lawson LM, Pare PD, Wiggs BJ, Kennedy S, Hogg JC. Morphology of peripheral airways in current smokers and ex-smokers. The American review of respiratory disease. 1983;127(4):474-7. PubMed PMID: 6838053.

49. Rutgers SR, Postma DS, ten Hacken NH, Kauffman HF, van Der Mark TW, Koeter GH, et al. Ongoing airway inflammation in patients with COPD who do not currently smoke. Thorax. 2000;55(1):12-8. PubMed PMID: 10607796; PubMed Central PMCID: PMC1745599.

50. Cosio MG, Saetta M, Agusti A. Immunologic aspects of chronic obstructive pulmonary disease. The New England journal of medicine. 2009;360(23):2445-54. doi: 10.1056/NEJMra0804752. PubMed PMID: 19494220.

51. Richens TR, Linderman DJ, Horstmann SA, Lambert C, Xiao YQ, Keith RL, et al. Cigarette smoke impairs clearance of apoptotic cells through oxidant-dependent activation of RhoA. American journal of respiratory and critical care medicine. 2009;179(11):1011-21. doi: 10.1164/rccm.200807-1148OC. PubMed PMID: 19264974; PubMed Central PMCID: PMC2689911.

52. Tuder RM, Petrache I. Pathogenesis of chronic obstructive pulmonary disease. The Journal of clinical investigation. 2012;122(8):2749-55. doi: 10.1172/JCI60324. PubMed PMID: 22850885; PubMed Central PMCID: PMC3408733.

53. Hogan BL, Barkauskas CE, Chapman HA, Epstein JA, Jain R, Hsia CC, et al. Repair and regeneration of the respiratory system: complexity, plasticity, and mechanisms of lung stem cell function. Cell stem cell. 2014;15(2):123-38. doi: 10.1016/j.stem.2014.07.012. PubMed PMID: 25105578; PubMed Central PMCID: PMC4212493.

54. Crystal RG. Airway basal cells. The "smoking gun" of chronic obstructive pulmonary disease. American journal of respiratory and critical care medicine. 2014;190(12):1355-62. doi: 10.1164/rccm.201408-1492PP. PubMed PMID: 25354273; PubMed Central PMCID: PMC4299651.

55. Knowles MR, Boucher RC. Mucus clearance as a primary innate defense mechanism for mammalian airways. The Journal of clinical investigation. 2002;109(5):571-7. doi: 10.1172/JCI15217. PubMed PMID: 11877463; PubMed Central PMCID: PMC150901.

56. Tilley AE, Walters MS, Shaykhiev R, Crystal RG. Cilia dysfunction in lung disease. Annual review of physiology. 2015;77:379-406. doi: 10.1146/annurev-physiol-021014-071931. PubMed PMID: 25386990; PubMed Central PMCID: PMC4465242.

57. Rock JR, Onaitis MW, Rawlins EL, Lu Y, Clark CP, Xue Y, et al. Basal cells as stem cells of the mouse trachea and human airway epithelium. Proceedings of the National Academy of Sciences of the United States of America. 2009;106(31):12771-5. doi: 10.1073/pnas.0906850106. PubMed PMID: 19625615; PubMed Central PMCID: PMC2714281.

58. Tata PR, Mou H, Pardo-Saganta A, Zhao R, Prabhu M, Law BM, et al. Dedifferentiation of committed epithelial cells into stem cells *in vivo*. Nature. 2013;503(7475):218-23. doi: 10.1038/nature12777. PubMed PMID: 24196716; PubMed Central PMCID: PMC4035230.

59. Blanpain C, Fuchs E. Stem cell plasticity. Plasticity of epithelial stem cells in tissue regeneration. Science. 2014;344(6189):1242281. doi: 10.1126/science.1242281. PubMed PMID: 24926024; PubMed Central PMCID: PMC4523269.

60. Auerbach O, Stout AP, Hammond EC, Garfinkel L. Changes in bronchial epithelium in relation to cigarette smoking and in relation to lung cancer. The New England journal of medicine. 1961;265:253-67. doi: 10.1056/NEJM196108102650601. PubMed PMID: 13685078.

61. Polosukhin VV, Cates JM, Lawson WE, Zaynagetdinov R, Milstone AP, Massion PP, et al. Bronchial secretory immunoglobulin a deficiency correlates with airway inflammation and progression of chronic obstructive pulmonary disease. American journal of respiratory and critical care medicine. 2011;184(3):317-27. doi: 10.1164/rccm.201010-1629OC. PubMed PMID: 21512171; PubMed Central PMCID: PMC3265275.

62. Foster WM, Langenback EG, Bergofsky EH. Disassociation in the mucociliary function of central and peripheral airways of asymptomatic smokers. The American review of respiratory disease. 1985;132(3):633-9. doi: 10.1164/arrd.1985.132.3.633. PubMed PMID: 2864009.

63. Heijink IH, Brandenburg SM, Postma DS, van Oosterhout AJ. Cigarette smoke impairs airway epithelial barrier function and cell-cell contact recovery. The European respiratory journal. 2012;39(2):419-28. doi: 10.1183/09031936.00193810. PubMed PMID: 21778164.

64. Staudt MR, Buro-Auriemma LJ, Walters MS, Salit J, Vincent T, Shaykhiev R, et al. Airway Basal stem/progenitor cells have diminished capacity to regenerate airway epithelium in chronic obstructive pulmonary disease. American journal of respiratory and critical care medicine. 2014;190(8):955-8. doi: 10.1164/rccm.201406-1167LE. PubMed PMID: 25317467; PubMed Central PMCID: PMC4299582.

65. Ganesan S, Comstock AT, Sajjan US. Barrier function of airway tract epithelium. Tissue barriers. 2013;1(4):e24997. doi: 10.4161/tisb.24997. PubMed PMID: 24665407; PubMed Central PMCID: PMC3783221.

66. Whitsett JA, Alenghat T. Respiratory epithelial cells orchestrate pulmonary innate immunity. Nature immunology. 2015;16(1):27-35. doi: 10.1038/ni.3045. PubMed PMID: 25521682; PubMed Central PMCID: PMC4318521.

67. Gohy ST, Hupin C, Pilette C, Ladjemi MZ. Chronic inflammatory airway diseases: the central role of the epithelium revisited. Clinical and experimental allergy : journal of the British Society for Allergy and Clinical Immunology. 2016;46(4):529-42. doi: 10.1111/cea.12712. PubMed PMID: 27021118.

68. Parker D, Prince A. Innate immunity in the respiratory epithelium. American journal of respiratory cell and molecular biology. 2011;45(2):189-201. doi: 10.1165/rcmb.2011-0011RT. PubMed PMID: 21330463; PubMed Central PMCID: PMC3175551.

69. Kaetzel CS. The polymeric immunoglobulin receptor: bridging innate and adaptive immune responses at mucosal surfaces. Immunological reviews. 2005;206:83-99. doi: 10.1111/j.0105-2896.2005.00278.x. PubMed PMID: 16048543.

70. Woof JM, Russell MW. Structure and function relationships in IgA. Mucosal immunology. 2011;4(6):590-7. doi: 10.1038/mi.2011.39. PubMed PMID: 21937984.

71. Kaetzel CS. Cooperativity among secretory IgA, the polymeric immunoglobulin receptor, and the gut microbiota promotes host-microbial mutualism. Immunology letters. 2014;162(2 Pt A):10-21. doi: 10.1016/j.imlet.2014.05.008. PubMed PMID: 24877874; PubMed Central PMCID: PMC4246051.

72. Mantis NJ, Rol N, Corthesy B. Secretory IgA's complex roles in immunity and mucosal homeostasis in the gut. Mucosal immunology. 2011;4(6):603-11. doi: 10.1038/mi.2011.41. PubMed PMID: 21975936; PubMed Central PMCID: PMC3774538.

73. Pabst O. New concepts in the generation and functions of IgA. Nature reviews Immunology. 2012;12(12):821-32. doi: 10.1038/nri3322. PubMed PMID: 23103985.

74. Corthesy B. Role of secretory IgA in infection and maintenance of homeostasis. Autoimmunity reviews. 2013;12(6):661-5. doi: 10.1016/j.autrev.2012.10.012. PubMed PMID: 23201924.

75. Casanova JE, Breitfeld PP, Ross SA, Mostov KE. Phosphorylation of the polymeric immunoglobulin receptor required for its efficient transcytosis. Science. 1990;248(4956):742-5. PubMed PMID: 2110383.

76. Casanova JE, Apodaca G, Mostov KE. An autonomous signal for basolateral sorting in the cytoplasmic domain of the polymeric immunoglobulin receptor. Cell. 1991;66(1):65-75. PubMed PMID: 2070419.

77. Mostov K, Apodaca G, Aroeti B, Okamoto C. Plasma membrane protein sorting in polarized epithelial cells. The Journal of cell biology. 1992;116(3):577-83. PubMed PMID: 1730769; PubMed Central PMCID: PMC2289323.

78. Okamoto CT, Shia SP, Bird C, Mostov KE, Roth MG. The cytoplasmic domain of the polymeric immunoglobulin receptor contains two internalization signals that are distinct from its basolateral sorting signal. The Journal of biological chemistry. 1992;267(14):9925-32. PubMed PMID: 1577823.

79. Okamoto CT, Song W, Bomsel M, Mostov KE. Rapid internalization of the polymeric immunoglobulin receptor requires phosphorylated serine 726. The Journal of biological chemistry. 1994;269(22):15676-82. PubMed PMID: 8195218.

80. Luton F, Verges M, Vaerman JP, Sudol M, Mostov KE. The SRC family protein tyrosine kinase p62yes controls polymeric IgA transcytosis *in vivo*. Molecular cell. 1999;4(4):627-32. PubMed PMID: 10549294.

81. van ISC, Tuvim MJ, Weimbs T, Dickey BF, Mostov KE. Direct interaction between Rab3b and the polymeric immunoglobulin receptor controls ligand-stimulated transcytosis in epithelial cells. Developmental cell. 2002;2(2):219-28. PubMed PMID: 11832247.

82. Mostov KE, Altschuler Y, Chapin SJ, Enrich C, Low SH, Luton F, et al. Regulation of protein traffic in polarized epithelial cells: the polymeric immunoglobulin receptor model. Cold Spring Harbor symposia on quantitative biology. 1995;60:775-81. PubMed PMID: 8824452.

83. Kaetzel, C. S. 2013. The Polymeric Immunoglobulin Receptor. eLS.

84. Pilette C, Ouadrhiri Y, Godding V, Vaerman JP, Sibille Y. Lung mucosal immunity: immunoglobulin-A revisited. The European respiratory journal. 2001;18(3):571-88. PubMed PMID: 11589357.

85. Pilette C, Godding V, Kiss R, Delos M, Verbeken E, Decaestecker C, et al. Reduced epithelial expression of secretory component in small airways correlates with airflow obstruction in chronic obstructive pulmonary disease. American journal of respiratory and critical care medicine. 2001;163(1):185-94. doi: 10.1164/ajrccm.163.1.9912137. PubMed PMID: 11208645.

86. Pilette C, Durham SR, Vaerman JP, Sibille Y. Mucosal immunity in asthma and chronic obstructive pulmonary disease: a role for immunoglobulin A? Proceedings of the American Thoracic Society. 2004;1(2):125-35. doi: 10.1513/pats.2306032. PubMed PMID: 16113425.

87. Gohy ST, Detry BR, Lecocq M, Bouzin C, Weynand BA, Amatngalim GD, et al. Polymeric immunoglobulin receptor down-regulation in chronic obstructive pulmonary disease. Persistence in the cultured epithelium and role of transforming growth factor-beta. American journal of respiratory and critical care medicine. 2014;190(5):509-21. doi: 10.1164/rccm.201311-1971OC. PubMed PMID: 25078120.

88. Du RH, Richmond BW, Blackwell TS, Jr., Cates JM, Massion PP, Ware LB, et al. Secretory IgA from submucosal glands does not compensate for its airway surface deficiency in chronic obstructive pulmonary disease. Virchows Archiv : an international journal of pathology. 2015. doi: 10.1007/s00428-015-1854-0. PubMed PMID: 26432569.

89. Corthesy B. Roundtrip ticket for secretory IgA: role in mucosal homeostasis? Journal of immunology. 2007;178(1):27-32. PubMed PMID: 17182536.

90. Reikvam DH, Derrien M, Islam R, Erofeev A, Grcic V, Sandvik A, et al. Epithelial-microbial crosstalk in polymeric Ig receptor deficient mice. European journal of immunology. 2012;42(11):2959-70. doi: 10.1002/eji.201242543. PubMed PMID: 22865203.

91. Mestecky J, Russell MW, Jackson S, Brown TA. The human IgA system: a reassessment. Clinical immunology and immunopathology. 1986;40(1):105-14. PubMed PMID: 2424650.

92. Conley ME, Delacroix DL. Intravascular and mucosal immunoglobulin A: two separate but related systems of immune defense? Annals of internal medicine. 1987;106(6):892-9. PubMed PMID: 3579073.

93. Berg RD, Savage DC. Immune responses of specific pathogen-free and gnotobiotic mice to antigens of indigenous and nonindigenous microorganisms. Infection and immunity. 1975;11(2):320-9. PubMed PMID: 1089600; PubMed Central PMCID: PMC415064.

94. Slack E, Balmer ML, Fritz JH, Hapfelmeier S. Functional flexibility of intestinal IgA - broadening the fine line. Frontiers in immunology. 2012;3:100. doi: 10.3389/fimmu.2012.00100. PubMed PMID: 22563329; PubMed Central PMCID: PMC3342566.

95. Sun K, Johansen FE, Eckmann L, Metzger DW. An important role for polymeric Ig receptor-mediated transport of IgA in protection against Streptococcus pneumoniae nasopharyngeal carriage. Journal of immunology. 2004;173(7):4576-81. PubMed PMID: 15383591.

96. Tjarnlund A, Rodriguez A, Cardona PJ, Guirado E, Ivanyi J, Singh M, et al. Polymeric IgR knockout mice are more susceptible to mycobacterial infections in the respiratory tract than

wild-type mice. International immunology. 2006;18(5):807-16. doi: 10.1093/intimm/dxl017. PubMed PMID: 16569672.

97. Cunningham KA, Carey AJ, Finnie JM, Bao S, Coon C, Jones R, et al. Poly-immunoglobulin receptor-mediated transport of IgA into the male genital tract is important for clearance of Chlamydia muridarum infection. American journal of reproductive immunology. 2008;60(5):405-14. doi: 10.1111/j.1600-0897.2008.00637.x. PubMed PMID: 18803626.

98. Sixbey JW, Yao QY. Immunoglobulin A-induced shift of Epstein-Barr virus tissue tropism. Science. 1992;255(5051):1578-80. PubMed PMID: 1312750.

99. Zhang JR, Mostov KE, Lamm ME, Nanno M, Shimida S, Ohwaki M, et al. The polymeric immunoglobulin receptor translocates pneumococci across human nasopharyngeal epithelial cells. Cell. 2000;102(6):827-37. PubMed PMID: 11030626.

100. Cunningham-Rundles C. Physiology of IgA and IgA deficiency. Journal of clinical immunology. 2001;21(5):303-9. PubMed PMID: 11720003.

101. Moon C, Baldridge MT, Wallace MA, Burnham CA, Virgin HW, Stappenbeck TS. Vertically transmitted faecal IgA levels determine extra-chromosomal phenotypic variation. Nature. 2015;521(7550):90-3. doi: 10.1038/nature14139. PubMed PMID: 25686606; PubMed Central PMCID: PMC4425643.

102. van der Waaij LA, Limburg PC, Mesander G, van der Waaij D. *In vivo* IgA coating of anaerobic bacteria in human faeces. Gut. 1996;38(3):348-54. PubMed PMID: 8675085; PubMed Central PMCID: PMC1383061.

103. Suzuki K, Meek B, Doi Y, Muramatsu M, Chiba T, Honjo T, et al. Aberrant expansion of segmented filamentous bacteria in IgA-deficient gut. Proceedings of the National Academy of

Sciences of the United States of America. 2004;101(7):1981-6. doi: 10.1073/pnas.0307317101. PubMed PMID: 14766966; PubMed Central PMCID: PMC357038.

104. Cullender TC, Chassaing B, Janzon A, Kumar K, Muller CE, Werner JJ, et al. Innate and adaptive immunity interact to quench microbiome flagellar motility in the gut. Cell host & microbe. 2013;14(5):571-81. doi: 10.1016/j.chom.2013.10.009. PubMed PMID: 24237702; PubMed Central PMCID: PMC3920589.

105. Mirpuri J, Raetz M, Sturge CR, Wilhelm CL, Benson A, Savani RC, et al. Proteobacteria-specific IgA regulates maturation of the intestinal microbiota. Gut microbes. 2014;5(1):28-39. doi: 10.4161/gmic.26489. PubMed PMID: 24637807; PubMed Central PMCID: PMC4049932.

106. Palm NW, de Zoete MR, Cullen TW, Barry NA, Stefanowski J, Hao L, et al. Immunoglobulin A coating identifies colitogenic bacteria in inflammatory bowel disease. Cell. 2014;158(5):1000-10. doi: 10.1016/j.cell.2014.08.006. PubMed PMID: 25171403; PubMed Central PMCID: PMC4174347.

107. Bunker JJ, Flynn TM, Koval JC, Shaw DG, Meisel M, McDonald BD, et al. Innate and Adaptive Humoral Responses Coat Distinct Commensal Bacteria with Immunoglobulin A. Immunity. 2015;43(3):541-53. doi: 10.1016/j.immuni.2015.08.007. PubMed PMID: 26320660; PubMed Central PMCID: PMC4575282.

108. Frantz AL, Rogier EW, Weber CR, Shen L, Cohen DA, Fenton LA, et al. Targeted deletion of MyD88 in intestinal epithelial cells results in compromised antibacterial immunity associated with downregulation of polymeric immunoglobulin receptor, mucin-2, and antibacterial peptides. Mucosal immunology. 2012;5(5):501-12. doi: 10.1038/mi.2012.23. PubMed PMID: 22491177; PubMed Central PMCID: PMC3422608.

109. Polosukhin VV, Richmond BW, Du RH, Cates JM, Wu P, Nian H, et al. SIgA Deficiency in Individual Small Airways is Associated with Persistent Inflammation and Remodeling. American journal of respiratory and critical care medicine. 2016. doi: 10.1164/rccm.201604-0759OC. PubMed PMID: 27911098.

110. Hempen PM, Phillips KM, Conway PS, Sandoval KH, Schneeman TA, Wu HJ, et al. Transcriptional regulation of the human polymeric Ig receptor gene: analysis of basal promoter elements. Journal of immunology. 2002;169(4):1912-21. PubMed PMID: 12165516.

111. Bruno ME, West RB, Schneeman TA, Bresnick EH, Kaetzel CS. Upstream stimulatory factor but not c-Myc enhances transcription of the human polymeric immunoglobulin receptor gene. Molecular immunology. 2004;40(10):695-708. PubMed PMID: 14644095.

112. Kvale D, Brandtzaeg P, Lovhaug D. Up-regulation of the expression of secretory component and HLA molecules in a human colonic cell line by tumour necrosis factor-alpha and gamma interferon. Scandinavian journal of immunology. 1988;28(3):351-7. PubMed PMID: 3143150.

113. Ackermann LW, Wollenweber LA, Denning GM. IL-4 and IFN-gamma increase steady state levels of polymeric Ig receptor mRNA in human airway and intestinal epithelial cells. Journal of immunology. 1999;162(9):5112-8. PubMed PMID: 10227981.

114. Ackermann LW, Denning GM. Nuclear factor-kappaB contributes to interleukin-4- and interferon-dependent polymeric immunoglobulin receptor expression in human intestinal epithelial cells. Immunology. 2004;111(1):75-85. PubMed PMID: 14678201; PubMed Central PMCID: PMC1782392.

115. Mueller R, Chanez P, Campbell AM, Bousquet J, Heusser C, Bullock GR. Different cytokine patterns in bronchial biopsies in asthma and chronic bronchitis. Respiratory medicine. 1996;90(2):79-85. PubMed PMID: 8730325.

116. Chung KF. Cytokines in chronic obstructive pulmonary disease. The European respiratory journal Supplement. 2001;34:50s-9s. PubMed PMID: 12392035.

117. Marshall CB, Mays DJ, Beeler JS, Rosenbluth JM, Boyd KL, Santos Guasch GL, et al. p73 Is Required for Multiciliogenesis and Regulates the Foxj1-Associated Gene Network. Cell reports. 2016;14(10):2289-300. doi: 10.1016/j.celrep.2016.02.035. PubMed PMID: 26947080; PubMed Central PMCID: PMC4794398.

118. Nemajerova A, Kramer D, Siller SS, Herr C, Shomroni O, Pena T, et al. TAp73 is a central transcriptional regulator of airway multiciliogenesis. Genes & development. 2016;30(11):1300-12. doi: 10.1101/gad.279836.116. PubMed PMID: 27257214; PubMed Central PMCID: PMC4911929.

119. Johansen FE, Pekna M, Norderhaug IN, Haneberg B, Hietala MA, Krajci P, et al. Absence of epithelial immunoglobulin A transport, with increased mucosal leakiness, in polymeric immunoglobulin receptor/secretory component-deficient mice. The Journal of experimental medicine. 1999;190(7):915-22. PubMed PMID: 10510081; PubMed Central PMCID: PMC2195652.

120. Han W, Zaynagetdinov R, Yull FE, Polosukhin VV, Gleaves LA, Tanjore H, et al. Molecular Imaging of Folate Receptor Beta Positive Macrophages During Acute Lung Inflammation. American journal of respiratory cell and molecular biology. 2014. doi: 10.1165/rcmb.2014-0289OC. PubMed PMID: 25375039.

121. Caporaso JG, Kuczynski J, Stombaugh J, Bittinger K, Bushman FD, Costello EK, et al. QIIME allows analysis of high-throughput community sequencing data. Nature methods. 2010;7(5):335-6. doi: 10.1038/nmeth.f.303. PubMed PMID: 20383131; PubMed Central PMCID: PMC3156573.

122. Richmond BW, Brucker RM, Han W, Du RH, Zhang Y, Cheng DS, et al. Airway bacteria drive a progressive COPD-like phenotype in mice with polymeric immunoglobulin receptor deficiency. Nature communications. 2016;7:11240. doi: 10.1038/ncomms11240. PubMed PMID: 27046438; PubMed Central PMCID: PMC4822073.

123. Vestbo J, Hurd SS, Agusti AG, Jones PW, Vogelmeier C, Anzueto A, et al. Global strategy for the diagnosis, management, and prevention of chronic obstructive pulmonary disease: GOLD executive summary. American journal of respiratory and critical care medicine. 2013;187(4):347-65. doi: 10.1164/rccm.201204-0596PP. PubMed PMID: 22878278.

124. McDonough JE, Yuan R, Suzuki M, Seyednejad N, Elliott WM, Sanchez PG, et al. Small-airway obstruction and emphysema in chronic obstructive pulmonary disease. The New England journal of medicine. 2011;365(17):1567-75. doi: 10.1056/NEJMoa1106955. PubMed PMID: 22029978; PubMed Central PMCID: PMC3238466.

125. Baraldo S, Turato G, Saetta M. Pathophysiology of the small airways in chronic obstructive pulmonary disease. Respiration; international review of thoracic diseases. 2012;84(2):89-97. doi: 10.1159/000341382. PubMed PMID: 22868355.

126. Decramer M, Janssens W, Miravitlles M. Chronic obstructive pulmonary disease. Lancet. 2012;379(9823):1341-51. doi: 10.1016/S0140-6736(11)60968-9. PubMed PMID: 22314182.

127. Johansen FE, Kaetzel CS. Regulation of the polymeric immunoglobulin receptor and IgA transport: new advances in environmental factors that stimulate pIgR expression and its role in mucosal immunity. Mucosal immunology. 2011;4(6):598-602. doi: 10.1038/mi.2011.37. PubMed PMID: 21956244; PubMed Central PMCID: PMC3196803.

128. Polosukhin VV. Ultrastructural of the bronchial epithelium in chronic inflammation. Ultrastructural pathology. 2001;25(2):119-28. PubMed PMID: 11407525.

129. Shimada S, Kawaguchi-Miyashita M, Kushiro A, Sato T, Nanno M, Sako T, et al. Generation of polymeric immunoglobulin receptor-deficient mouse with marked reduction of secretory IgA. Journal of immunology. 1999;163(10):5367-73. PubMed PMID: 10553061.

130. Shapiro SD. The pathogenesis of emphysema: the elastase:antielastase hypothesis 30 years later. Proceedings of the Association of American Physicians. 1995;107(3):346-52. PubMed PMID: 8608421.

131. Shifren A, Mecham RP. The stumbling block in lung repair of emphysema: elastic fiber assembly. Proceedings of the American Thoracic Society. 2006;3(5):428-33. doi: 10.1513/pats.200601-009AW. PubMed PMID: 16799087; PubMed Central PMCID: PMC2658707.

132. Churg A, Wright JL. Proteases and emphysema. Current opinion in pulmonary medicine. 2005;11(2):153-9. PubMed PMID: 15699789.

133. Lungarella G, Cavarra E, Lucattelli M, Martorana PA. The dual role of neutrophil elastase in lung destruction and repair. The international journal of biochemistry & cell biology. 2008;40(6-7):1287-96. doi: 10.1016/j.biocel.2007.12.008. PubMed PMID: 18243764.

134. Mocchegiani E, Giacconi R, Costarelli L. Metalloproteases/anti-metalloproteases imbalance in chronic obstructive pulmonary disease: genetic factors and treatment implications. Current opinion in pulmonary medicine. 2011;17 Suppl 1:S11-9. doi: 10.1097/01.mcp.0000410743.98087.12. PubMed PMID: 22209925.

135. Hoenderdos K, Condliffe A. The neutrophil in chronic obstructive pulmonary disease. American journal of respiratory cell and molecular biology. 2013;48(5):531-9. doi: 10.1165/rcmb.2012-0492TR. PubMed PMID: 23328639.

136. Vermeulen L, De Wilde G, Van Damme P, Vanden Berghe W, Haegeman G. Transcriptional activation of the NF-kappaB p65 subunit by mitogen- and stress-activated protein kinase-1 (MSK1). The EMBO journal. 2003;22(6):1313-24. doi: 10.1093/emboj/cdg139. PubMed PMID: 12628924; PubMed Central PMCID: PMC151081.

137. Darb-Esfahani S, Sinn BV, Weichert W, Budczies J, Lehmann A, Noske A, et al. Expression of classical NF-kappaB pathway effectors in human ovarian carcinoma. Histopathology. 2010;56(6):727-39. doi: 10.1111/j.1365-2559.2010.03544.x. PubMed PMID: 20546338.

138. Law M, Corsino P, Parker NT, Law BK. Identification of a small molecule inhibitor of serine 276 phosphorylation of the p65 subunit of NF-kappaB using in silico molecular docking. Cancer letters. 2010;291(2):217-24. doi: 10.1016/j.canlet.2009.10.015. PubMed PMID: 19910110; PubMed Central PMCID: PMC2849932.

139. Barfod KK, Roggenbuck M, Hansen LH, Schjorring S, Larsen ST, Sorensen SJ, et al. The murine lung microbiome in relation to the intestinal and vaginal bacterial communities. BMC microbiology. 2013;13:303. doi: 10.1186/1471-2180-13-303. PubMed PMID: 24373613; PubMed Central PMCID: PMC3878784.

140. Knights D, Costello EK, Knight R. Supervised classification of human microbiota. FEMS microbiology reviews. 2011;35(2):343-59. doi: 10.1111/j.1574-6976.2010.00251.x. PubMed PMID: 21039646.

141. Finney LJ, Ritchie A, Pollard E, Johnston SL, Mallia P. Lower airway colonization and inflammatory response in COPD: a focus on Haemophilus influenzae. International journal of chronic obstructive pulmonary disease. 2014;9:1119-32. doi: 10.2147/COPD.S54477. PubMed PMID: 25342897; PubMed Central PMCID: PMC4206200.

142. Van Eldere J, Slack MP, Ladhani S, Cripps AW. Non-typeable Haemophilus influenzae, an under-recognised pathogen. The Lancet Infectious diseases. 2014;14(12):1281-92. doi: 10.1016/S1473-3099(14)70734-0. PubMed PMID: 25012226.

143. Martorana PA, Beume R, Lucattelli M, Wollin L, Lungarella G. Roflumilast fully prevents emphysema in mice chronically exposed to cigarette smoke. American journal of respiratory and critical care medicine. 2005;172(7):848-53. doi: 10.1164/rccm.200411-1549OC. PubMed PMID: 15961691.

144. Martorana PA, Lunghi B, Lucattelli M, De Cunto G, Beume R, Lungarella G. Effect of roflumilast on inflammatory cells in the lungs of cigarette smoke-exposed mice. BMC pulmonary medicine. 2008;8:17. doi: 10.1186/1471-2466-8-17. PubMed PMID: 18755021; PubMed Central PMCID: PMC2533284.

145. Michalski JM, Golden G, Ikari J, Rennard SI. PDE4: a novel target in the treatment of chronic obstructive pulmonary disease. Clinical pharmacology and therapeutics. 2012;91(1):134-42. doi: 10.1038/clpt.2011.266. PubMed PMID: 22130119.

146. Tashkin DP. Roflumilast : the new orally active, selective phophodiesterase-4 inhibitor, for the treatment of COPD. Expert opinion on pharmacotherapy. 2014;15(1):85-96. doi: 10.1517/14656566.2013.837159. PubMed PMID: 24032576.

147. Rinaldi M, Maes K, De Vleeschauwer S, Thomas D, Verbeken EK, Decramer M, et al. Long-term nose-only cigarette smoke exposure induces emphysema and mild skeletal muscle dysfunction in mice. Disease models & mechanisms. 2012;5(3):333-41. doi: 10.1242/dmm.008508. PubMed PMID: 22279084; PubMed Central PMCID: PMC3339827.

148. Schneeman TA, Bruno ME, Schjerven H, Johansen FE, Chady L, Kaetzel CS. Regulation of the polymeric Ig receptor by signaling through TLRs 3 and 4: linking innate and adaptive immune responses. Journal of immunology. 2005;175(1):376-84. PubMed PMID: 15972671.

149. Pinner NA, Hamilton LA, Hughes A. Roflumilast: a phosphodiesterase-4 inhibitor for the treatment of severe chronic obstructive pulmonary disease. Clinical therapeutics. 2012;34(1):56-66. doi: 10.1016/j.clinthera.2011.12.008. PubMed PMID: 22284994.

150. Ganesan S, Comstock AT, Kinker B, Mancuso P, Beck JM, Sajjan US. Combined exposure to cigarette smoke and nontypeable Haemophilus influenzae drives development of a COPD phenotype in mice. Respiratory research. 2014;15:11. doi: 10.1186/1465-9921-15-11. PubMed PMID: 24495712; PubMed Central PMCID: PMC3926338.

151. Primary immunodeficiency diseases. Report of a WHO Scientific Group. Clinical and experimental immunology. 1995;99 Suppl 1:1-24. PubMed PMID: 7813117; PubMed Central PMCID: PMC1534127.

152. Brandtzaeg P, Karlsson G, Hansson G, Petruson B, Bjorkander J, Hanson LA. The clinical condition of IgA-deficient patients is related to the proportion of IgD- and IgM-producing cells in their nasal mucosa. Clinical and experimental immunology. 1987;67(3):626-36. PubMed PMID: 3301101; PubMed Central PMCID: PMC1542640.

153. Klemola T. Immunohistochemical findings in the intestine of IgA-deficient persons: number of intraepithelial T lymphocytes is increased. Journal of pediatric gastroenterology and nutrition. 1988;7(4):537-43. PubMed PMID: 3294370.

154. Hsia CC, Hyde DM, Ochs M, Weibel ER, Structure AEJTFoQAoL. An official research policy statement of the American Thoracic Society/European Respiratory Society: standards for quantitative assessment of lung structure. American journal of respiratory and critical care medicine. 2010;181(4):394-418. doi: 10.1164/rccm.200809-1522ST. PubMed PMID: 20130146.

155. Zaynagetdinov R, Stathopoulos GT, Sherrill TP, Cheng DS, McLoed AG, Ausborn JA, et al. Epithelial nuclear factor-kappaB signaling promotes lung carcinogenesis via recruitment of regulatory T lymphocytes. Oncogene. 2012;31(26):3164-76. doi: 10.1038/onc.2011.480. PubMed PMID: 22002309; PubMed Central PMCID: PMC3266969.

156. Webster GA, Perkins ND. Transcriptional cross talk between NF-kappaB and p53. Molecular and cellular biology. 1999;19(5):3485-95. PubMed PMID: 10207072; PubMed Central PMCID: PMC84141.

157. Kikuchi H, Ozaki T, Furuya K, Hanamoto T, Nakanishi M, Yamamoto H, et al. NF-kappaB regulates the stability and activity of p73 by inducing its proteolytic degradation through a ubiquitin-dependent proteasome pathway. Oncogene. 2006;25(58):7608-17. doi: 10.1038/sj.onc.1209748. PubMed PMID: 16953234.

158. Cheng DS, Han W, Chen SM, Sherrill TP, Chont M, Park GY, et al. Airway epithelium controls lung inflammation and injury through the NF-kappa B pathway. Journal of immunology. 2007;178(10):6504-13. PubMed PMID: 17475880.

159. Tiwary R, Yu W, Sanders BG, Kline K. alpha-TEA cooperates with chemotherapeutic agents to induce apoptosis of p53 mutant, triple-negative human breast cancer cells via activating p73. Breast cancer research : BCR. 2011;13(1):R1. doi: 10.1186/bcr2801. PubMed PMID: 21214929; PubMed Central PMCID: PMC3109563.

160. O'Shaughnessy TC, Ansari TW, Barnes NC, Jeffery PK. Inflammation in bronchial biopsies of subjects with chronic bronchitis: inverse relationship of CD8+ T lymphocytes with FEV1. American journal of respiratory and critical care medicine. 1997;155(3):852-7. doi: 10.1164/ajrccm.155.3.9117016. PubMed PMID: 9117016.

161. Saetta M, Di Stefano A, Turato G, Facchini FM, Corbino L, Mapp CE, et al. CD8+ T-lymphocytes in peripheral airways of smokers with chronic obstructive pulmonary disease. American journal of respiratory and critical care medicine. 1998;157(3 Pt 1):822-6. doi: 10.1164/ajrccm.157.3.9709027. PubMed PMID: 9517597.

162. Saetta M, Baraldo S, Corbino L, Turato G, Braccioni F, Rea F, et al. CD8+ve cells in the lungs of smokers with chronic obstructive pulmonary disease. American journal of respiratory and critical care medicine. 1999;160(2):711-7. doi: 10.1164/ajrccm.160.2.9812020. PubMed PMID: 10430750.

163. Retamales I, Elliott WM, Meshi B, Coxson HO, Pare PD, Sciurba FC, et al. Amplification of inflammation in emphysema and its association with latent adenoviral infection. American journal of respiratory and critical care medicine. 2001;164(3):469-73. doi: 10.1164/ajrccm.164.3.2007149. PubMed PMID: 11500352.

164. van der Strate BW, Postma DS, Brandsma CA, Melgert BN, Luinge MA, Geerlings M, et al. Cigarette smoke-induced emphysema: A role for the B cell? American journal of respiratory and critical care medicine. 2006;173(7):751-8. doi: 10.1164/rccm.200504-594OC. PubMed PMID: 16399994.